Long-term wave response

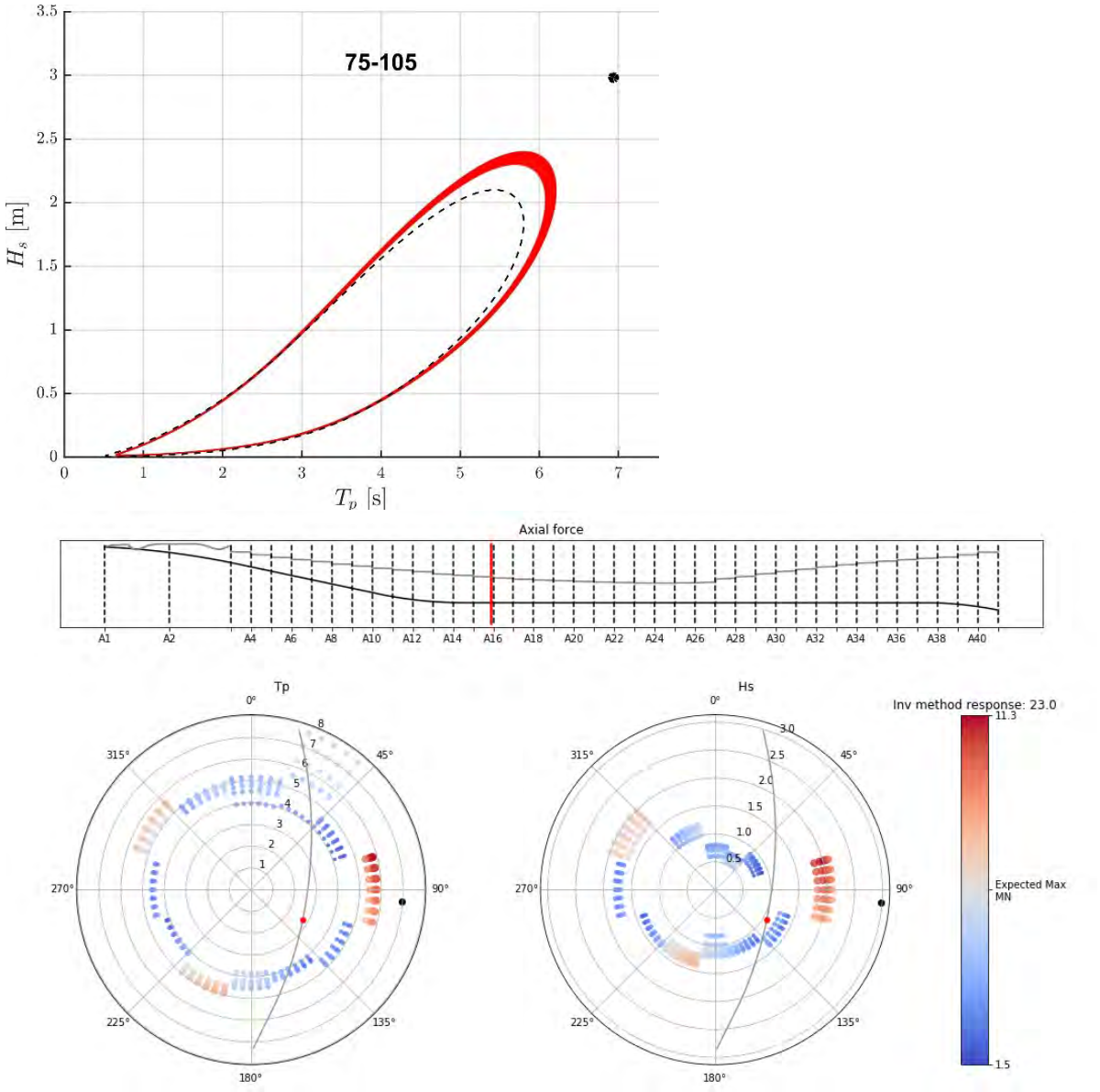

Figure 3-21: Case 9. Axial force in the bridge girder at the south side of axis 16 for 100-year return period sea states along the contour, plotted together with the IFORM design point (black dot). The IFORM response is indicated above the colour bar. The top figure shows the IFORM design point along with the environmental contours for the relevant sector, cf. Figure 2-3.

Long-term wave response

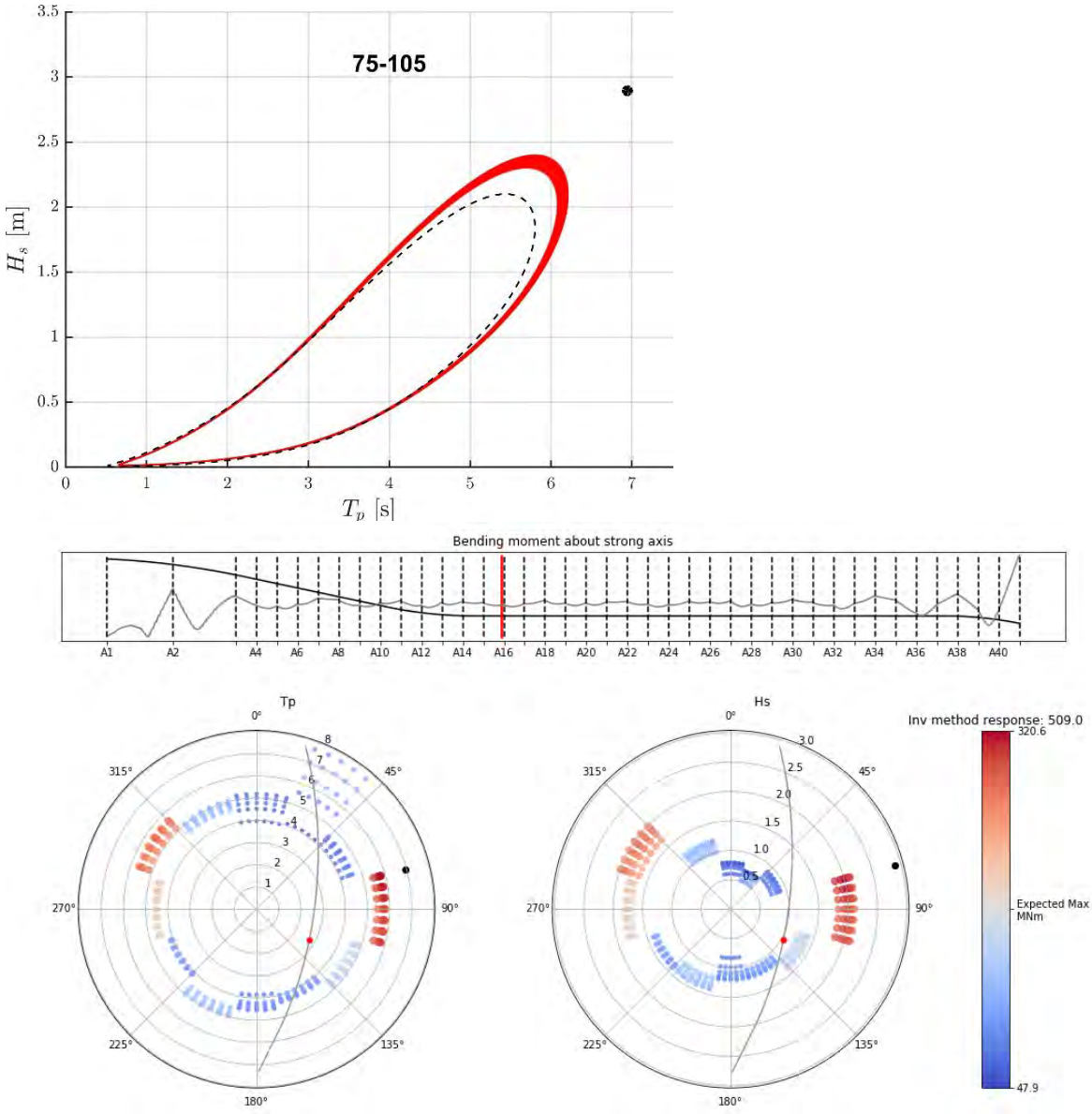

Figure 3-22: Case 10. Bending moment about strong axis in the bridge girder at the south side of axis 16 for 100-year return period sea states along the contour, plotted together with the IFORM design point (black dot). The IFORM response is indicated above the colour bar. The top figure shows the IFORM design point along with the environmental contours for the relevant sector, cf. Figure 2-3.

Long-term wave response

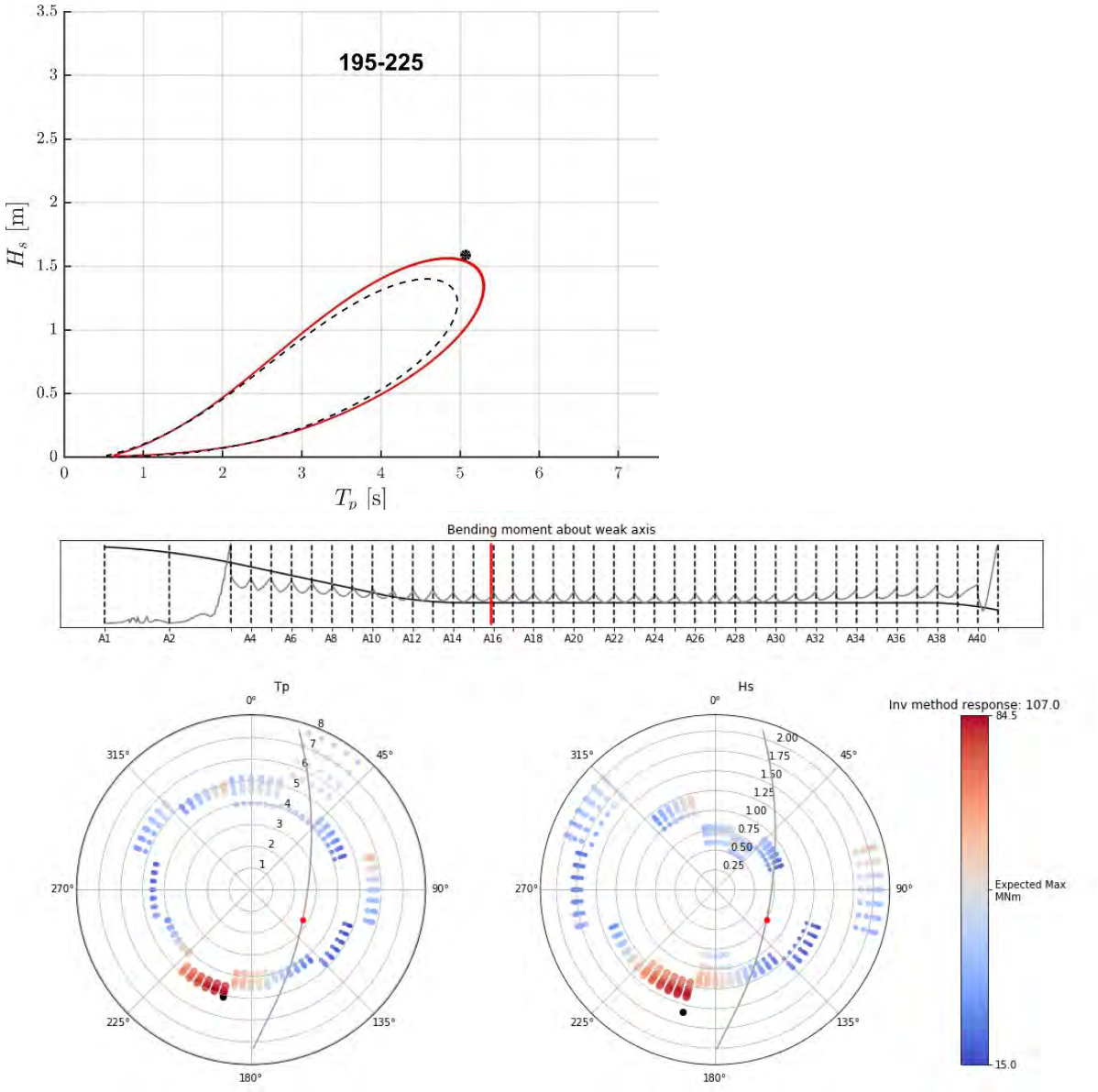

Figure 3-23: Case 11. Bending moment about weak axis in the bridge girder at the south side of axis 16 for 100-year return period sea states along the contour, plotted together with the IFORM design point (black dot). The IFORM response is indicated above the colour bar. The top figure shows the IFORM design point along with the environmental contours for the relevant sector, cf. Figure 2-3.

Long-term wave response

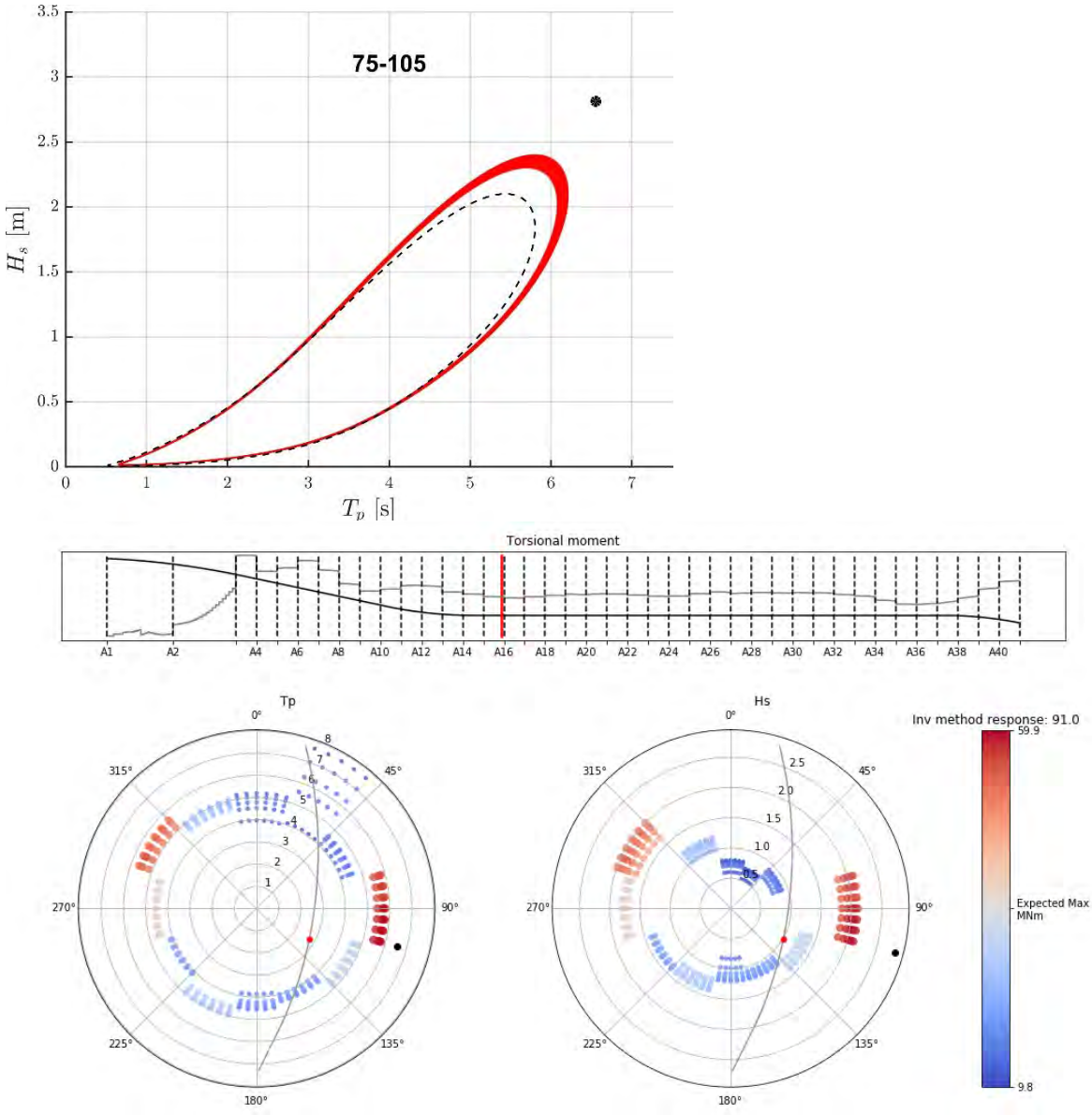

Figure 3-24: Case 12. Torsional moment in the bridge girder at the south side of axis 16 for 100-year return period sea states along the contour, plotted together with the IFORM design point (black dot). The IFORM response is indicated above the colour bar. The top figure shows the IFORM design point along with the environmental contours for the relevant sector, cf. Figure 2-3.

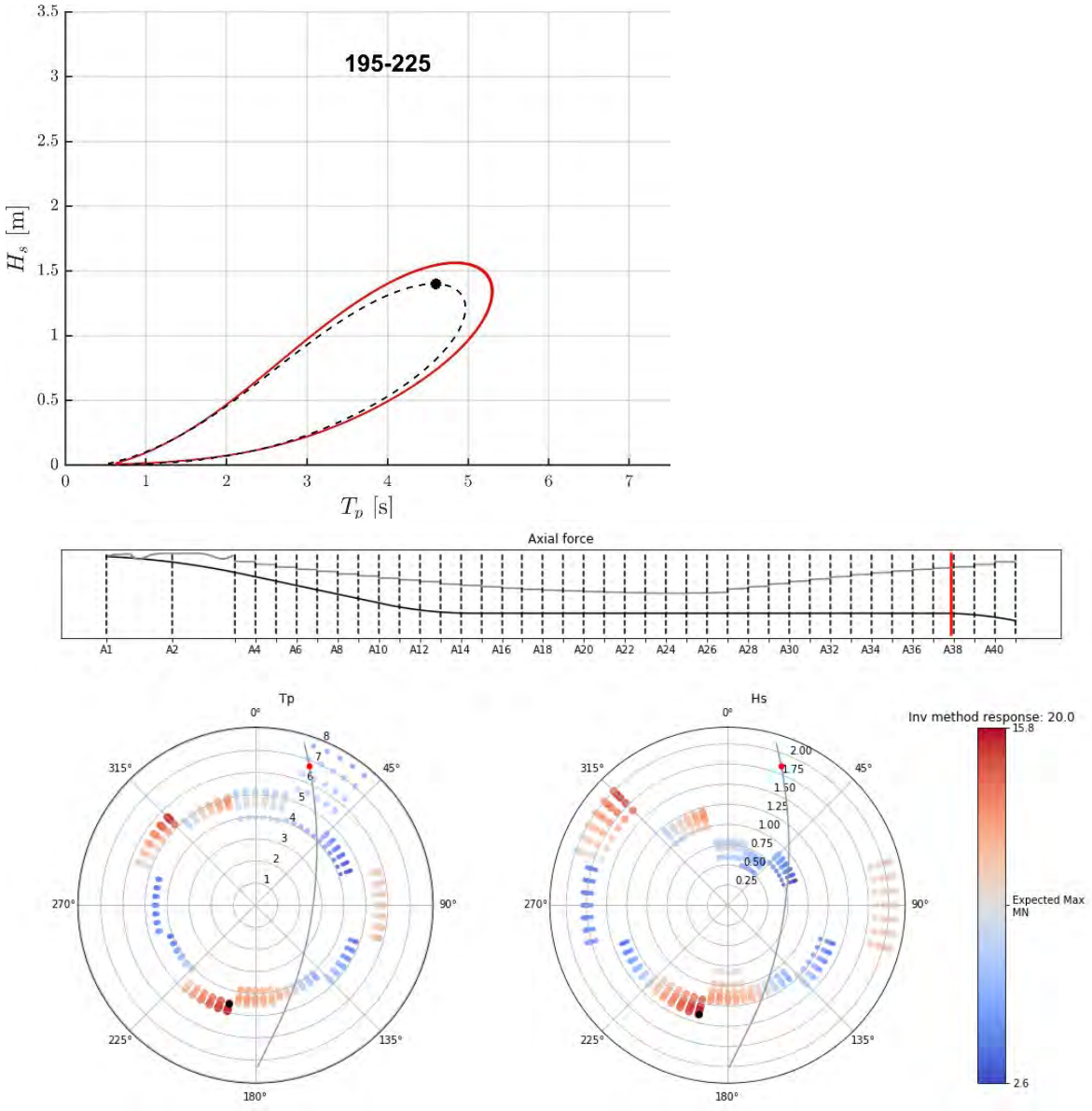

Figure 3-25: Case 13. Axial force in the bridge girder at the south side of axis 38 for 100-year return period sea states along the contour, plotted together with the IFORM design point (black dot). The IFORM response is indicated above the colour bar. The top figure shows the IFORM design point along with the environmental contours for the relevant sector, cf. Figure 2-3.

Long-term wave response

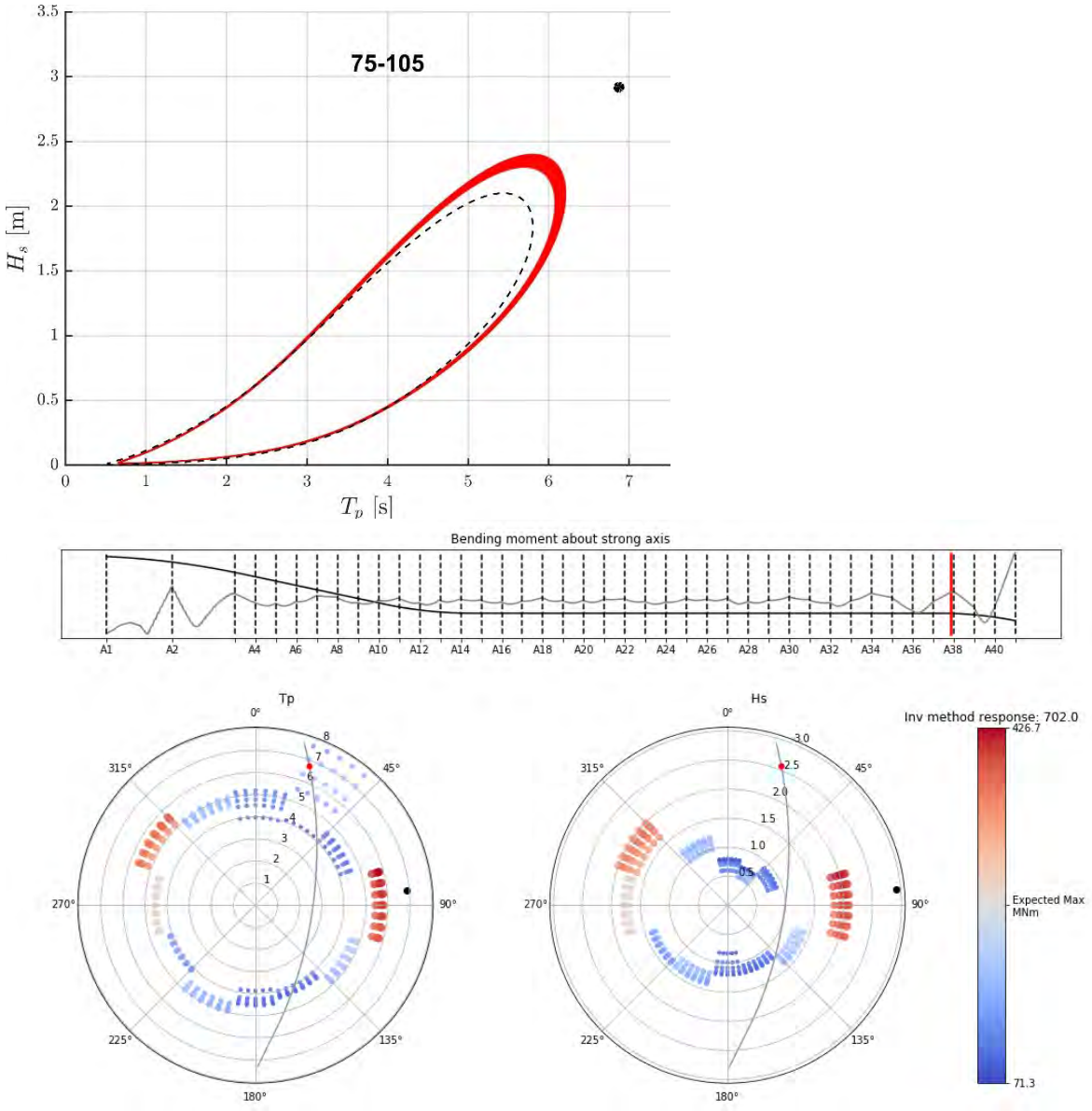

Figure 3-26: Case 14. Bending moment about strong axis in the bridge girder at the south side of axis 38 for 100-year return period sea states along the contour, plotted together with the IFORM design point (black dot). The IFORM response is indicated above the colour bar. The top figure shows the IFORM design point along with the environmental contours for the relevant sector, cf. Figure 2-3.

Long-term wave response

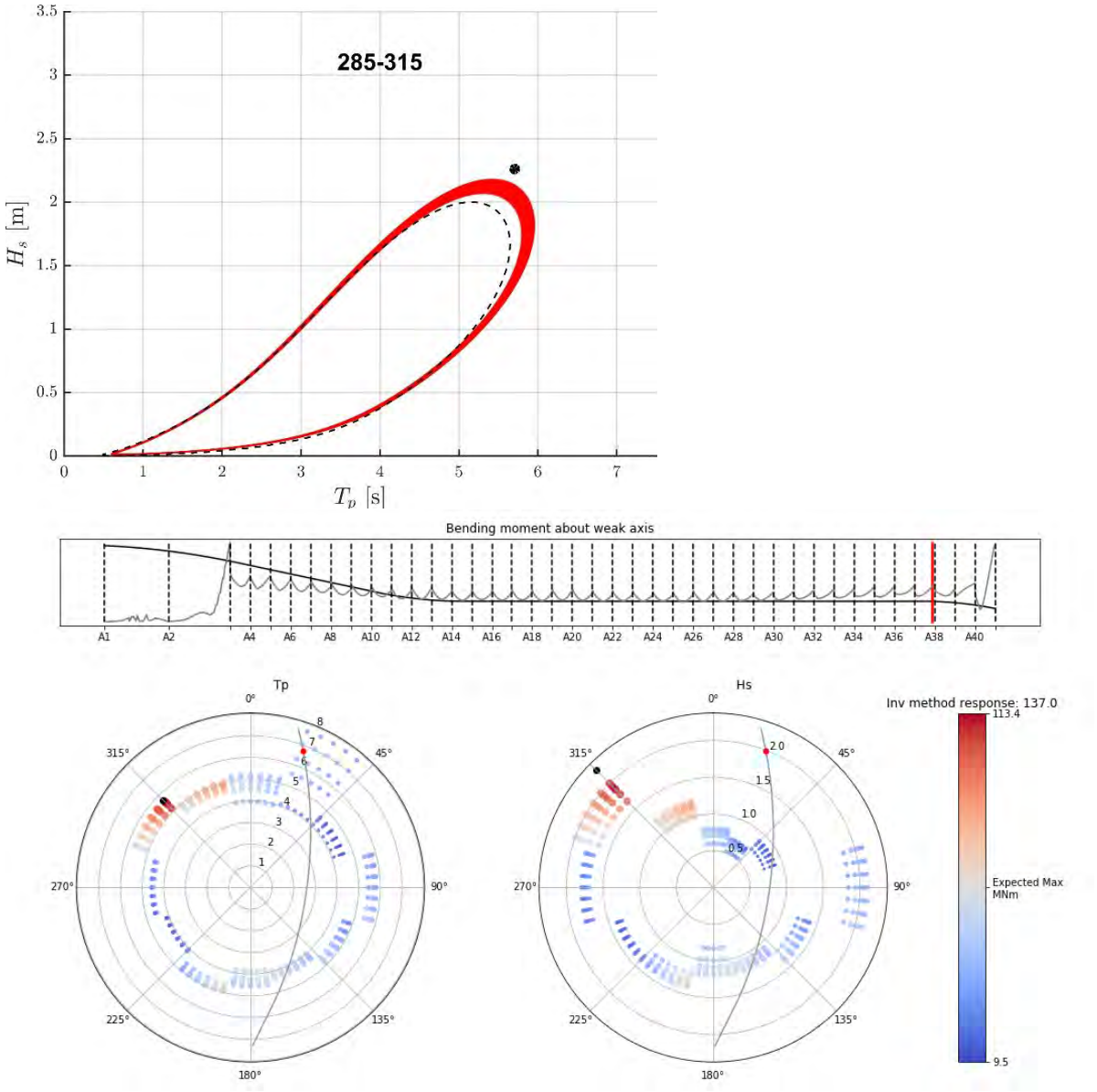

Figure 3-27: Case 15. Bending moment about weak axis in the bridge girder at the south side of axis 38 for 100-year return period sea states along the contour, plotted together with the IFORM design point (black dot). The IFORM response is indicated above the colour bar. The top figure shows the IFORM design point along with the environmental contours for the relevant sector, cf. Figure 2-3.

Long-term wave response

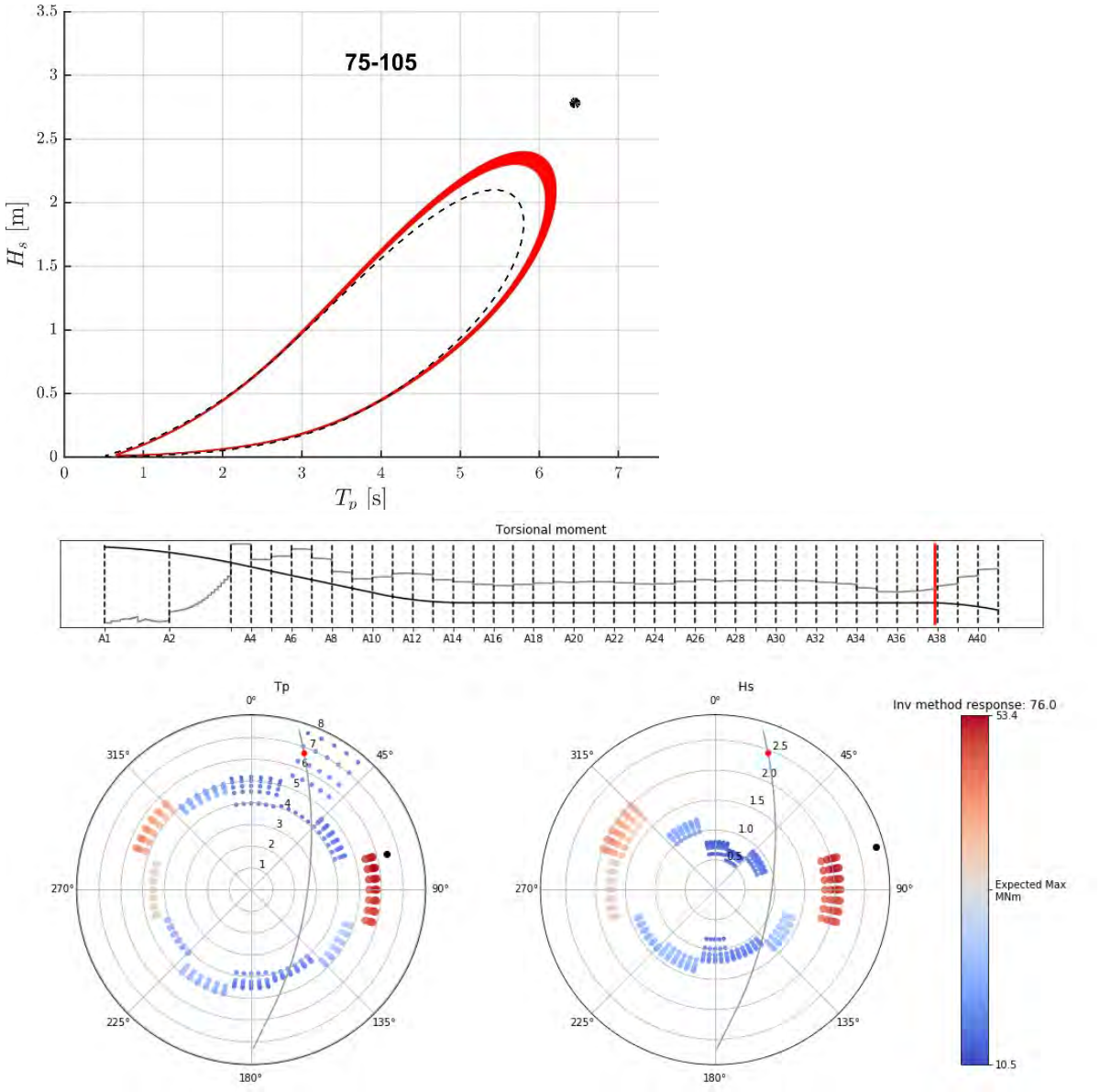

Figure 3-28: Case 16. Torsional moment in the bridge girder at the south side of axis 38 for 100-year return period sea states along the contour, plotted together with the IFORM design point (black dot). The IFORM response is indicated above the colour bar. The top figure shows the IFORM design point along with the environmental contours for the relevant sector, cf. Figure 2-3.

Long-term wave response

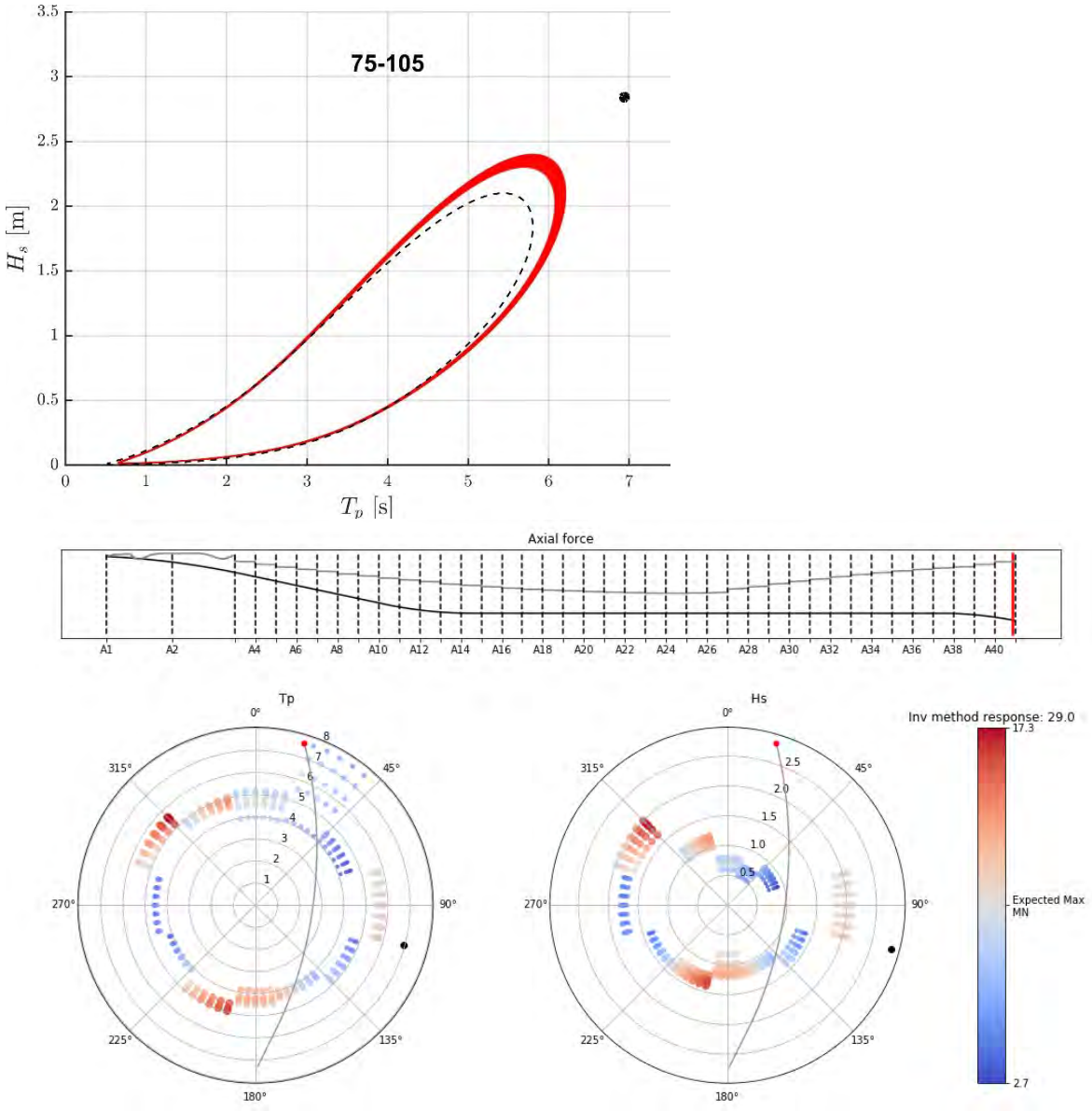

Figure 3-29: Case 17. Axial force in the bridge girder at the south side of axis 41 (north abutment) for 100-year return period sea states along the contour, plotted together with the IFORM design point (black dot). The IFORM response is indicated above the colour bar. The top figure shows the IFORM design point along with the environmental contours for the relevant sector, cf. Figure 2-3.

Long-term wave response

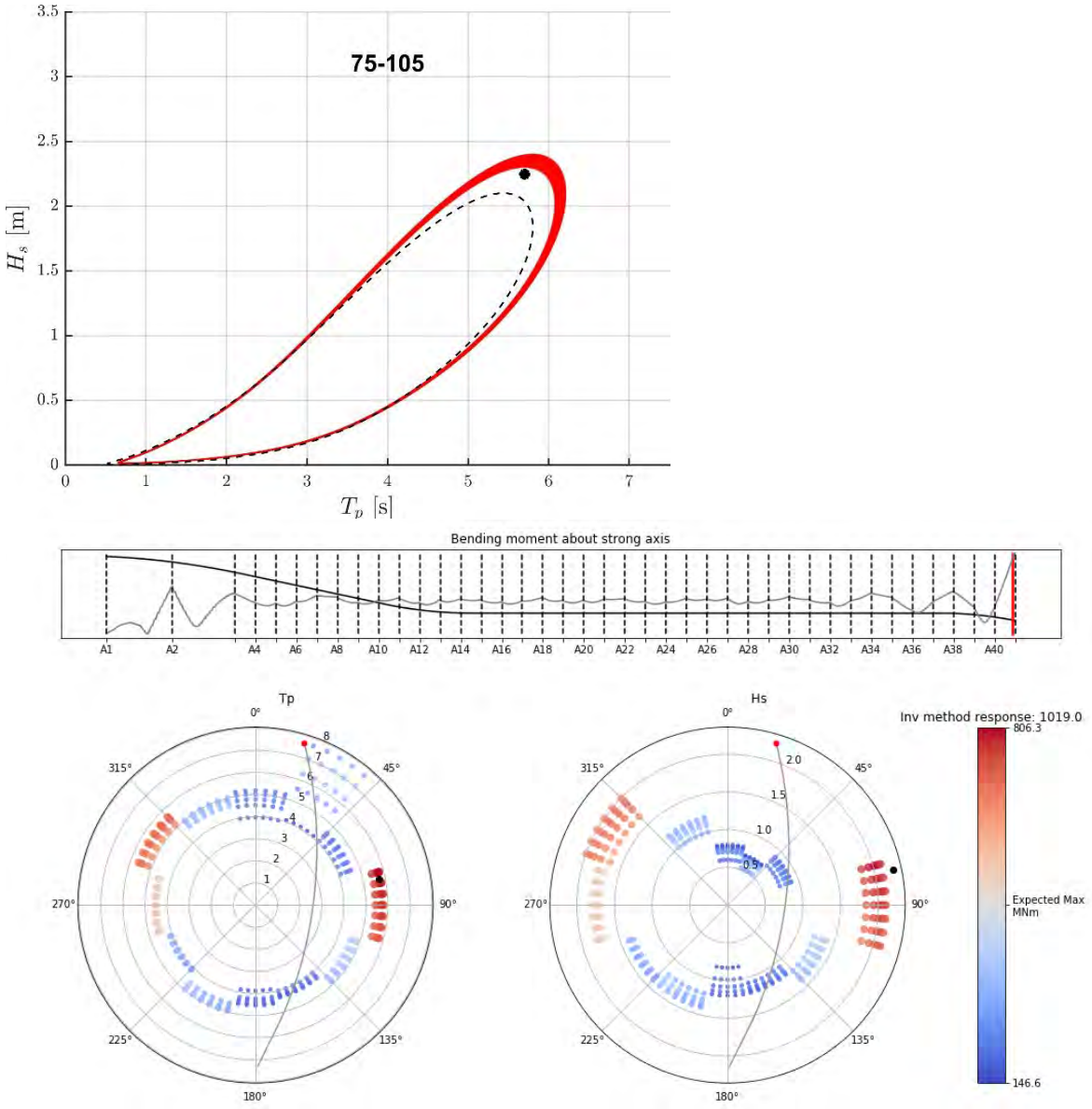

Figure 3-30: Case 18. Bending moment about strong axis in the bridge girder at the south side of axis 41 (north abutment) for 100-year return period sea states along the contour, plotted together with the IFORM design point (black dot). The IFORM response is indicated above the colour bar. The top figure shows the IFORM design point along with the environmental contours for the relevant sector, cf. Figure 2-3.

Long-term wave response

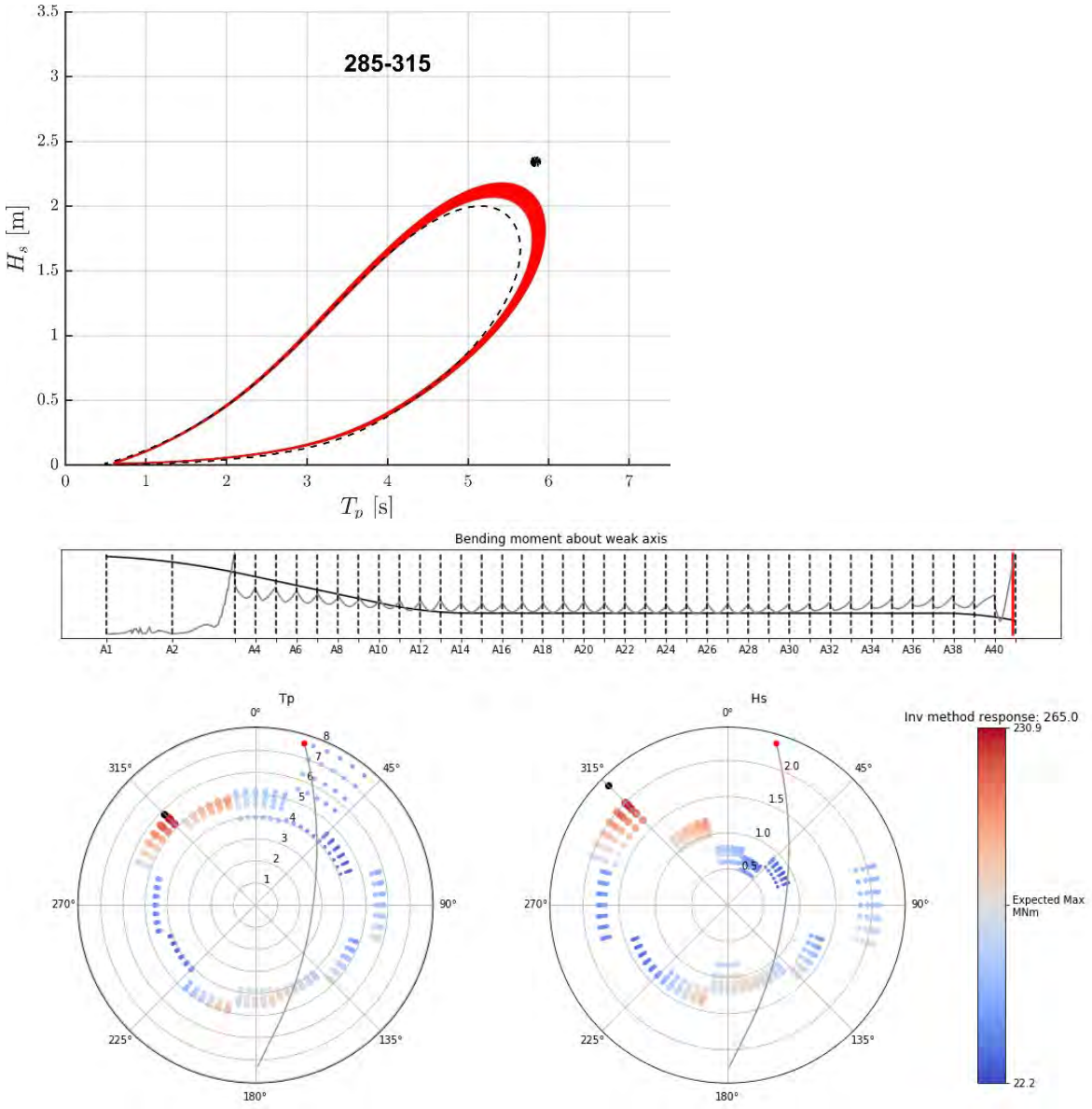

Figure 3-31: Case 19. Bending moment about weak axis in the bridge girder at the south side of axis 41 (north abutment) for 100-year return period sea states along the contour, plotted together with the IFORM design point (black dot). The IFORM response is indicated above the colour bar. The top figure shows the IFORM design point along with the environmental contours for the relevant sector, cf. Figure 2-3.

Long-term wave response

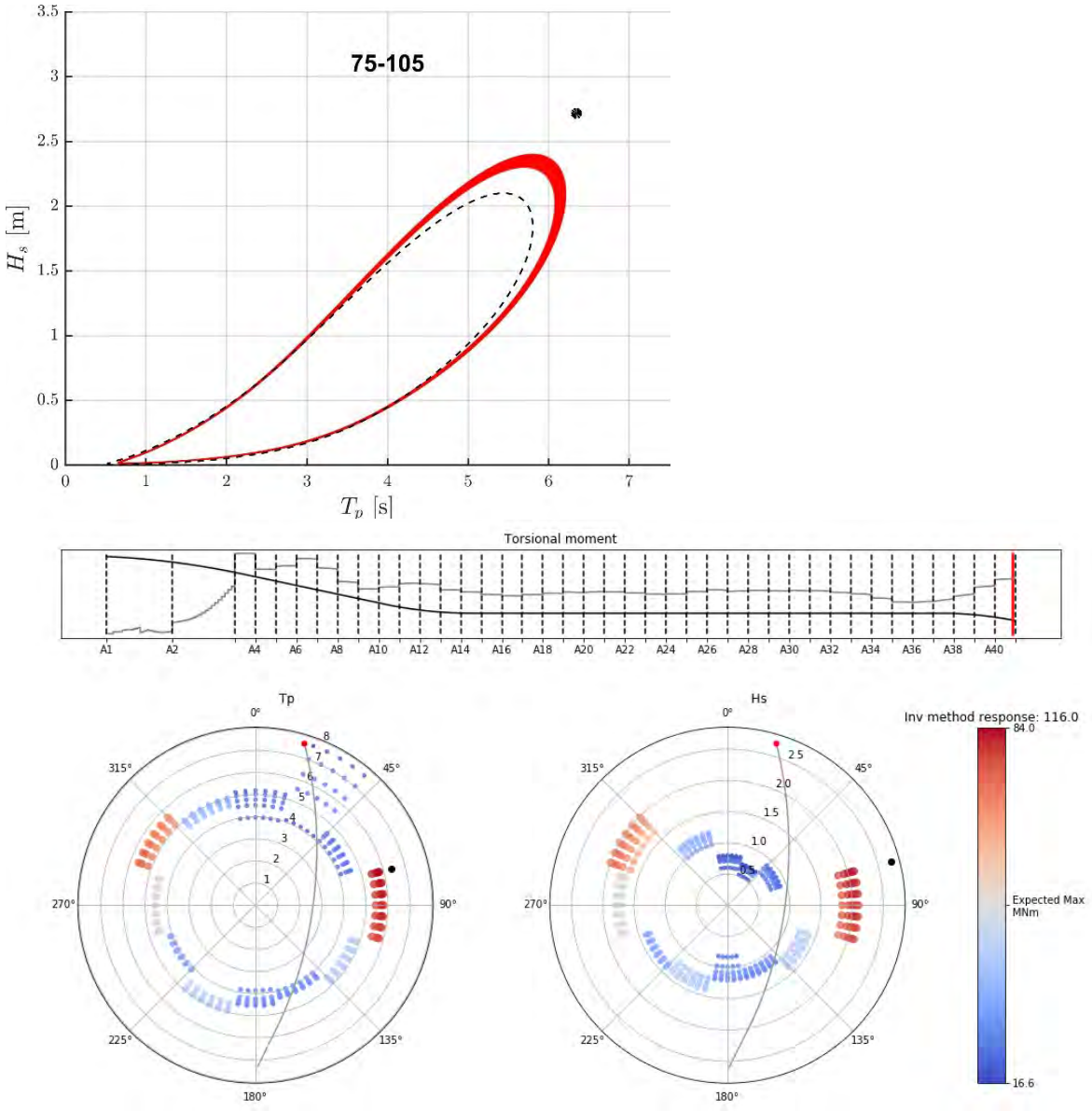

Figure 3-32: Case 20. Torsional moment in the bridge girder at the south side of axis 41 (north abutment) for 100-year return period sea states along the contour, plotted together with the IFORM design point (black dot). The IFORM response is indicated above the colour bar. The top figure shows the IFORM design point along with the environmental contours for the relevant sector, cf. Figure 2-3.

4 References

[1] A. Næss and M. Torgeir, Stochastic Dynamics of Marine Structures, Cambridge: Cambridge University Press, 2012.

[2] F.-I. G. Giske, "Long-Term Extreme Response Analysis of Marine Structures Using Inverse Reliability Methods," Norwegian University of Science and Technology (NTNU), Trondheim, 2017.

[3] F.-I. G. Giske, K.-A. Kvåle, B. J. Leira and O. Øiseth, "Long-term extreme response analysis of a long-span pontoon bridge," *Marine Structures,* vol. 58, pp. 154-171, 2018.

[4] Statens Vegvesen, "SBJ-01-C4-SVV-01-BA-001 MetOcean Design basis Rev. 1," 30.11.18.

[5] S. R. Winterstein, T. C. Ude, C. A. Cornell, P. Bjerager and S. Haver, "Environmental Parameters for Extreme Response: Inverse FORM with Omission Factors," in *Proc. 6th Int. Conf. on Structural Safety and Reliability*, Innsbruck, 1993.

[6] DNVGL, "DNVGL-RP-C205 Environmental Conditions and environmental loads," August 2017.

[7] E. Vanem, "A comparison study on the estimation of extreme structural response from different environmental contour methods," *Marine Structures,* vol. 56, pp. 137-162, 2017.

[8] W. Chai and B. J. Leira, "Environmental contours based on inverse SORM," *Marine Structures,* vol. 60, pp. 34-51, 2018.

[9] E. Ross, O. C. Astrup, E. Bitner-Gregersen, N. Bunn, G. Feld, B. Gouldby, A. Huseby, Y. Liu, D. Randell, E. Vanem and P. Jonathan, "On environmental contours for marine and coastal design," in *Proceedings of the ASME 2019 38th International Conference on Ocean, Offshore and Arctic Engineering (OMAE 2019)*, Glasgow, 2019.

[10] G. Feld, P. Jonathan and D. Randell, "On the estimation and application of directional design criteria," in *Proceedings of the ASME 2019 38th International Conference on Ocean, Offshore and Arctic Engineering (OMAE 2019)*, Glasgow, 2019.

Concept development, floating bridge E39 Bjørnafjorden

Appendix G – Enclosure 16

10205546-11-NOT-196

Uncertainty assessment

AAS-JAKOBSEN COWI Multiconsult

JOHS HOLT AkerSolutions entail NGI DISSING+WEITLING architecture a|s mossmaritime

Memo

PROJECT	Concept development, floating bridge E39 Bjørnafjorden	DOCUMENT CODE	10205546-11-NOT-196
CLIENT	Statens vegvesen	ACCESSIBILITY	Restricted
SUBJECT	Uncertainty assessment	PROJECT MANAGER	Svein Erik Jakobsen
TO		PREPARED BY	M. Storheim, F-C.W. Hanssen, K.A. Kvåle, F.-I. G. Giske, K. Aas-Jakobsen
COPY TO		RESPONSIBLE UNIT	

Summary

This memo discusses the work related to evaluation and mitigation of known uncertainties in the Bjørnafjorden floating bridge project. The uncertainty and measures taken to investigate the uncertainty is described, and the findings discussed.

0	15.08.2019	First issue	MS/FCWH/KAK/ FIGG/KAA	P. N. Larsen	S. E. Jakobsen
REV.	Date	Description	Prepared by	Checked by	Approved by

Uncertainty assessment

1. Introduction

This memo summarizes and discuss the work performed to reduce known uncertainties for the Bjørnafjorden floating bridge project, phase 5. Aspects related to the environmental design basis, hydrodynamic effects, analysis and modelling effects and parametric resonance were considered.

2. Environmental design basis

2.1. Uncertainties in the metocean contour line approach

2.1.1. Problem description

The ultimate goal of a long-term response analysis is to identify the response value with a given return period. More specifically, we seek the characteristic response value r_q, which has a specified annual exceedance probability q. This is referred to as the q-probability response or the $1/q$-year response.

The q-probability response is most accurately determined by a full long-term approach. However, due to the large computational cost associated with this approach, the environmental contour method is used to obtain reasonable estimates of the q-probability response. Recently, methods have been developed which provide more accurate estimates of the q-probability response at a significantly reduced computational cost [1, 2]. These methods are referred to as inverse reliability methods. The relation between the full long-term approach, the environmental contour method and the inverse reliability methods is explained in detail in a separate memo [3].

2.1.2. Performed investigation

In the Bjørnafjorden project so far, environmental contour lines have been applied to identify which sea states that give rise to the q-probability response. An assessment of the validity of the contour line approach is carried out in [3] for the concept K12_07. The 100-year response due to wind waves was calculated by an inverse reliability method, using joint distributions of Hs and Tp for each directional sector which were provided by the client. The provided (Hs,Tp)-distributions were the same distributions that the environmental contours reported in the metocean design basis are based on. However, the environmental contours that are reported therein have been adjusted in order to give more correct 100-year Hs values. Thus, the environmental model used with the inverse reliability method was not validated for direct use in a long-term response analysis. Still, the model was used to give an indication of the accuracy uncertainty of the contour line approach. The 100-year response due to wind waves was calculated for 20 different responses along the K12_07 concept using an inverse reliability method. The results were compared with the 100-year response estimates from the contour line approach.

2.1.3. Findings and recommendations

Even if the results in the performed investigation are based on an environmental model that is not validated for use in long-term response estimation, they give an indication that the estimates of the long-term response produced by the contour line approach might be too rough in some cases. It is however not possible to draw any definite conclusion without a comparison with a full long-term approach. Further studies on the long-term response are therefore recommended. An environmental model suited for use in long-term response analyses should be established, and full integration of the long-term response formulation should be carried out for some selected cases.

It is also important to be aware that environmental contours corresponding to a given return period are not uniquely defined. Different methods exist to produce them, and these can give quite different results [4, 5, 6], especially when sector dependence is included [7].

2.2. Sensitivity of response along the metocean contour lines

2.2.1. Problem description

For the estimation of long-term response with the environmental contour method, the design point should be taken as the point along the contour which gives the most severe response. It has been assumed that it is the point along the contour with the largest value of Hs that gives the most severe response. However, this may not be the case and therefore the validity of this assumption has been investigated.

2.2.2. Performed investigation

The validity of the max Hs assumption is checked by including more sea states on the contour line and comparing the sea states that maximizes the individual responses from this extensive screening (5 points along the contour) with the simplified screening (only the point with max Hs). Five sea states are selected for each contour line; maximum significant wave height, maximum peak period and three sea states in between. This investigation is presented in the memo [3].

2.2.3. Findings and recommendations

The maximum response is not found at the maximum Hs but rather at a somewhat higher period. As the eigenmodes are closely spaced in this area this indicates that a slight increase in the period excites a different eigenmode in which higher response is observed for a lower wave height. However, the error in the response is only a few percent on most cases and around 10 % for the worst cases.

2.3. Wind spectrum parameters

2.3.1. Problem description

Table 15 in Metocean Design Basis indicate that the measurements on site shows large variation in wind input parameters. The values are tabulated as P10, P50 and P90 values. It is not clear which to choose in design calculations. Including all possible variations of the parameters will lead to an ineffective design procedure.

2.3.2. Performed investigation

Since Table 15 values influence dynamic response due to wind, the effect of varying the following parameters has been studied: xLu, Au, cux and Cuy. The analysis was performed for wind response only and for all wind directions. P50 values were chosen as reference if not specified otherwise.

2.3.3. Findings and recommendations

For variation of xLu the standard deviation of the response follows the reference value within +/- 10%. Low and high xLu values give lowest response. The results indicate that the highest response value for this concept is for an xLu value in medium range.

For variation of Au the standard deviation follows the reference value within +/- 10%. The general trend is that increased Au values gives increased response.

For variation of Cux the standard deviation follows the reference value within +/- 10%. The effect of change of cux is small for wind perpendicular to the alignment and more pronounced as the wind comes along the alignment. The Cux value of 3.0 used in the reference case gives the highest value of the calculated cases and increase of Cux value gives reduced response.

The response is sensitive to changes of the Cuy parameter, particularly for wind perpendicular to the alignment. Lower value of Cuy gives higher response, and Cuy values below the P10 value of 6.4 will increase the standard deviation of the response with more than 20%. For skew wind, where the wind is more along the alignment, the effect is less pronounced.

The findings are not universally valid, as it will be dependent on eigenfrequencies of the structure compared to the spectral distribution of wind. In order to be able to do an effective design we recommend that:

- Wind data is studied to see if the spread of the P10-P90 values can be reduced
- Further analysis is performed on the selected concept to conclude on which parameters to use in design.

3. Hydrodynamics

3.1. Viscous Damping on Pontoon

3.1.1. Problem description

Establishing realistic viscous damping coefficients for the pontoons is a nontrivial task for several reasons. One is the shape of the pontoon that differs from shapes typically reported in the literature, another is the dependency on parameters such as the Reynolds number and the Keulegan-Carpenter (KC) number. Another matter is the fact that the damping in waves is different from that in still water.

3.1.2. Performed investigation

Two dedicated activities have been performed in order to estimate the viscous damping (neglecting the added damping in waves): 1) Estimating quadratic drag coefficients based on literature and 2) estimating quadratic drag coefficients from a computational fluid dynamics (CFD) analysis performed by Core Marine.

When estimated from literature, the procedure was to first determine a steady-flow drag coefficient in 2D, then to determine a 3D correction factor, then to determine the KC number and finally making a KC-dependent correction of the steady-flow drag coefficient.

When the drag coefficient is estimated from literature, it is always a question which flow regime that applies, meaning if the boundary layer is laminar, partially turbulent or fully turbulent. This has implications for the flow separation point from non-sharp boundaries. Another uncertainty when estimating drag coefficients from literature for an unconventional geometry is the definition of the KC number. What is the relevant length scale, is it the draught, the breadth or something else? This has implications for the interpretation of analytical/empirical data.

When estimating the drag coefficient from CFD, the main uncertainty is related to the adequacy of the numerical model. Several aspects may influence the obtained results, such as spatial and temporal discretization, the size of the domain, the turbulence modelling etc. These are addressed more thoroughly in Appendix H of the global analyses report [8].

From the literature study, a recommended drag coefficient of 0.3 was proposed. The CFD analysis indicates a steady-flow drag coefficient of 0.41. These two estimates are deemed to be in reasonable agreement. The CFD analysis shows a strong increase in the drag coefficient for small KC numbers, meaning that the drag coefficient is strongly influenced by the motion amplitude of the pontoon.

3.1.3. Findings and recommendations

By estimating the drag coefficient from two independent methods, a better understanding of the important physical parameters influencing it has been obtained. Furthermore, the results obtained from the CFD analysis appear to have a systematic dependence on the KC number, and with results for high values of KC converging towards the steady-flow value. There area however remaining uncertainties due to the limiting scope of the CFD analysis as well as the modelling approach. These are discussed in [8].

In order to further reduce this uncertainty and increase the accuracy of the viscous loading on the pontoon, it is recommended to do dedicated model tests in future phases. Since the drag forces are much smaller than the inertia forces, one must design these tests in a clever way so that the drag force can be extracted in a reliable manner. Furthermore, model tests can give additional information regarding possible added damping (and excitation) in waves. One should also do additional CFD studies, using the model tests to validate these. A properly validated CFD model enables more thorough parameter studies to be performed with increased confidence in the results.

3.2. Wave-Current Interaction

3.2.1. Problem description

When a current is present together with waves, the wave loads (both radiation and diffraction loads) are modified due to wave-current interaction effects. This modification consists in 1) a pure Doppler frequency shift because the wave encounter frequency depends on the current and 2) additional terms in the hydrodynamic problem to be solved that depends on both the velocity potential and the current speed.

3.2.2. Performed investigation

The wave-current interaction effects are investigated by performing numerical analysis with a single pontoon in Wasim, considering different combinations of wave and current directions as well as current speeds. The results are compared to Wadam results (where the effect of current is not considered in the hydrodynamic problem) with the encounter period modified due to a pure Doppler shift. This comparison was done to 1) validate the Wasim results for zero current speed and 2) to investigate the importance of wave-current interaction effects beyond this frequency shift.

The hydrodynamic transfer functions for wave excitation loads as well as radiation loads (added mass and damping) from the Wasim analysis were imported into the global OrcaFlex model in order to investigate the effect on global responses.

3.2.3. Findings and recommendations

The comparison between Wasim and Wadam analyses showed that wave-current interactions may have a significant effect on wave excitation loads beyond a pure frequency (Doppler) shift. The effect was more significant for sway and roll than for heave. The effect on added mass and damping was much less pronounced. Importing the Wasim transfer functions into OrcaFlex revealed an increase in global responses such as the strong axis moment. The effect of wave-current interactions is more severe for K13 than for K12. The analysis is however done only with a current speed of 1.5 m/s, assumed uniform over the span of the bridge, and with current either aligned with or opposite of the wave direction. In order to have a better understanding of the significance of wave-current interaction effects, more detailed metocean data is required. Information about the instantaneous spatial variation of current across the fjord as well as the joint distribution of wave and current directions is needed. In general, it is found that the wave-current interaction effects are more significant for the Bjørnafjorden bridge than for typical offshore projects, since the waves are both shorter and lower compared to the current velocity than in design sea states offshore. It is also a matter of fact that the global response of the bridge is sensitive to wave-current interaction effects, largely because different modes can be triggered depending on the encounter frequency.

Since wave-current interactions have an important effect that should be accounted for in the design, it is recommended to do a further effort to reduce the uncertainty in future phases of the project. This effort should consist in 1) obtaining more accurate metocean data with respect to the joint distribution of waves and current, 2) to validate and verify the numerical model through model tests for a single pontoon and 3) to do more extensive studies on the global bridge model in OrcaFlex. The present assessment of wave-current interaction effects in OrcaFlex is done solely in frequency domain. This assumption should be verified by doing additional studies in time domain. An additional difficulty in OrcaFlex is that the wave spectrum must be modified manually in order to shift its different frequency components. This operation is not straightforward in short-crested waves, and hence only long-crested waves are considered here. Future work should investigate how to properly scale wave spectra for short-crested sea states and further assess the importance of wave-current interaction effects in short-crested versus long-crested waves.

3.3. Inhomogenous Sea States

3.3.1. Problem description

In the analysis of stationary marine structures, we typically assume that the sea state is stationary over a certain amount of time, often three hours, which enables us to analyse the problem statistically in an efficient manner. The structures considered generally have a length scale that is comparable to the wavelength, so that spatial variations in the sea state can be neglected.

The Bjørnafjorden bridge, on the other hand, spans over a significant area, and in practice the wave field will have properties that change along the path of the bridge due to diffraction, dispersion, varying wind and current intensities etc. The result is referred to as an *inhomogeneous* sea state where e.g. the wave spectrum used to describe the irregular sea state may differ from one location to the other. It is not only the spectral quantities, such as the significant wave height and peak period that can differ, but also the shape of the wave spectrum and properties such as the wave spreading and correlation lengths.

3.3.2. Performed investigation

As a step towards understanding the consequences of inhomogeneous sea states, analyses are performed where the phase angle of the wave excitation loads for each pontoon has been chosen randomly. This effectively removes the correlation between wave excitation between individual pontoons, which is otherwise assumed to be perfect. One must be aware that while this method reduces the correlation between loading on individual pontoons, the wave spectrum is still similar for each pontoon. Hence, diffraction or dispersive effects are not fully accounted for. In another study, the wave height is modified along the span of the bridge in accordance with the data given in the metocean report. Although they do not give the complete picture, these approaches enable us to study efficiently the global response's sensitivity towards disturbing the homogenous assumption in terms of correlation and wave height. It has also led to a better principal understanding of the involved mechanisms.

3.3.3. Findings and recommendations

By considering the phase angle of the wave excitation loads on individual pontoons as a random variable, the maximum bending moments about the strong and weak axes, as well as the torsional moment, are reduced over the bridge span. However, if the responses are investigated for a fixed location along the bridge for various combinations of the direction, height and period of the incident waves, the conclusion is more complex. Even though the extreme response is reduced, the response for a certain wave direction and period may very well increase as a function of inhomogeneity. This shows that one must carefully assess the effect of inhomogeneous sea states on a consequence level. As an example, increasing the response at certain critical periods may increase the risk of parametric excitation. When the wave height was varied along the bridge, an increase in maximum bending moments was observed towards the bridge ends.

The studies performed show that spatial variations of wave properties along the bridge may have a significant influence on global responses that are hard to anticipate. Moreover, it cannot be concluded in general that neglecting these effects is conservative, and the effect of inhomogeneous sea states should be further analysed. In the present phase, the study has focused on maximum loads, while the consequences for fatigue life have not been explored. Furthermore, the focus has been on the phase of wave excitation loads and varying wave height. One should also consider, and possibly analyse, spatial changes in wave periods, wave spectra, wave spreading, wave direction and current. This is a comprehensive list of parameters, and rational ways to simplify the analysis matrix and to process results statistically are required. For such assessment to be meaningful, metocean data with detail level beyond what is presently available is required.

3.4. Hydrodynamic Interaction

3.4.1. Problem description

Structures in proximity to each other experience hydrodynamic interaction effects in their radiation loads (added mass and damping) as well as in wave excitation loads. One consequence is that the motion of one body introduces radiation loads on other bodies. If the number of structures in the hydrodynamic analysis is N_b, the dimension of the added mass and radiation-damping matrices become $(6N_b \times 6N_b)$. This has consequences for the computational efficiency. If all bridge pontoons were to be considered simultaneously, the CPU time would be excessive and the problem, if studied in time domain, likely prone to numerical instabilities.

3.4.2. Performed investigation

A study has been performed to determine the number of pontoons that are necessary to include in the multibody hydrodynamic analysis. Including more pontoons on either side than those significantly influencing the hydrodynamic loads on a pontoon is unnecessary and has adverse effects on the computational efficiency. The interaction between adjacent pontoons are related to resonant wave motion, or sloshing, that depends on the distance between adjacent pontoons both with respect to resonance periods and resonance-induced amplification. To assess the effect on global responses, the hydrodynamic coefficients from multibody analysis with span widths 100 m and 125 m, respectively, were imported into OrcaFlex for frequency domain analysis.

3.4.3. Findings and recommendations

The hydrodynamic analysis demonstrated that it is generally sufficient to consider three pontoons in a multibody analysis, i.e. to determine the loads on a pontoon it is enough to consider on adjacent pontoon on each side. Only small changes were observed by increasing the number of pontoons in the analysis to five or beyond. From the frequency domain OrcaFlex analysis, hydrodynamic interaction effects appear to either have little effect on or reduce the maximum bending moments about the strong axis. The bending moment about the weak axis is found to be more sensitive, especially with 100 m span width. The analysis indicates that hydrodynamic interaction effects may be more important in fatigue sea states than in ULS conditions.

The method used to study global responses in frequency domain is incomplete in the sense that some coupling terms are neglected. Future studies should consider global time domain analysis. This was also attempted here but failed due to instabilities/convergence issues related to the so-called retardation functions (the time domain equivalents of the frequency domain added mass and damping). More effort is required to overcome this issue. One possibility that was not addressed in [8] is to neglect certain terms that are not considered important for the physical response, but that nevertheless can generate numerical problems. This has indeed been the experience when working with side-by-side mooring of LNG vessels, where the gap between the bodies is smaller and the hydrodynamic interaction stronger. Another measure that may improve the retardation functions is to use a lid in the hydrodynamic analysis in Wamit, where artificial damping is added to the free surface in order to avoid unrealistic sloshing wave elevations. This is also known to have a beneficial effect on the convergence and stability of the time domain retardation functions. The damping associated with such lids is however in general sea state dependent, and a careful calibration against model tests is necessary in order to obtain realistic values. This should be considered as future work, i.e. performing model tests designed to investigate hydrodynamic interaction effects and to calibrate the lid damping coefficient in the Wamit analysis. Such model tests need to be carefully planned in order to be valuable. The calibrated time domain model will indicate whether the frequency-domain approach is appropriate. With a validated model, it is recommended to do further analysis to investigate the influence of hydrodynamic interaction effects on fatigue life for the chosen concept.

3.5. Second Order Effects

3.5.1. Problem description

Second-order effects may give rise to mean, difference-frequency and sum-frequency wave loads. The difference-frequency loads and sum-frequency loads give rise to low- and high-frequency loading, respectively, that may be important if they coincide with important resonance periods. The classical example involving difference-frequency excitation is resonant slowly-varying wave drift loads on a moored structure with high natural periods in surge, sway and yaw. A typical example of sum-frequency excitation is resonant heave motions of a TLP with natural heave period in the range 2-4 s. In order to compute these second order loads, a second order hydrodynamic analysis must be performed. This is much more time consuming and sensitive to mesh refinement than a "standard" first order analysis, and requires that the free surface is discretized in order to satisfy second order free-surface conditions. Slowly-varying loads are often approximated from the mean wave drift loads by using the Newman approximation. The mean wave drift loads can be obtained from a first order hydrodynamic analysis. The Newman approximation is therefore a popular and widely used simplifying assumption. In general, the Newman approximation is valid when the relevant natural periods are in the order of 100 s or more and when the water depth is not very shallow. Such approximate methods are not available or well-established for sum-frequency loads.

3.5.2. Performed investigation

A second-order hydrodynamic analysis in Wamit was performed to calculate transfer functions for difference-frequency loads (so-called full QTF) for a single pontoon without any current.

3.5.3. Findings and recommendations

The analysis performed in the present phase of the project indicated that Newman's approximation is sufficiently accurate to predict the slowly varying horizontal-plane excitation of the pontoons. There are however issues to be further clarified, such as the slowly-varying drift loads and damping of slowly-varying motions due to wave-current interaction effects. For the present project, the current is more significant relative to the water particle velocities than in traditional offshore applications, and it is not evident that traditional methods are valid. In order to study this in more detail, a combination of dedicated model tests and advanced numerical methods (either non-linear potential flow or CFD methods) are recommended. It should also be investigated if there are important viscous contributions to the slowly-varying wave loads, especially when the current speed is significant.

Sum-frequency loads have not been addressed in the present phase of the project. However, because the global bridge response has natural periods over a large period band from very small to large periods, one cannot conclude that these loads are not important. For instance, in a sea state with peak period $T_p = 6\ s$, there will be energetic wave components with e.g. periods $T = 5\ s$ and $T = 7\ s$ giving rise to sum-frequency loads with frequency $f = \frac{1}{7\ s} + \frac{1}{5\ s} = 0.343\ hz$, i.e. a period of approximately 2.9 s. It is possible that such difference-frequency loading, particularly in heave, roll and pitch, may induce global responses in the bridge, especially considering that the piston mode on the pontoons is in this period range (e.g., the mode in which every other pontoon goes up or down causing large weak-axis moments). It is therefore recommended to do a numerical study also of second-order sum-frequency effects in future phases of the project. In planning such study, one must be aware that sum-frequency effects can pose a numerical challenge with respect to convergence and stability. A thorough assessment of the numerical convergence is thus appropriate.

3.6. Freeboard exceedance

3.6.1. Problem description

If water exceeds the freeboard of one or several pontoons, loads that influence the global response of the bridge may occur. The pontoon freeboard is set to 3.5 m, so that the incident wave elevation or the pontoon motions alone are not enough to induce negative freeboard. However, one must consider the possibility that the combination of large sea states, pontoon motions, wave-current interaction effects and non-linear diffraction effects may lead to water exceeding the freeboard.

3.6.2. Performed investigation

Several alternatives were considered to model the effect of freeboard exceedance. One of these was to simply reduce the heave, roll and pitch restoring coefficients of the pontoon. This alternative was however considered inadequate, since 1) the restoring is related to the linear motion of the floater and not the relative wave elevation and 2) it does not reflect the fact that freeboard exceedance is a transient phenomenon and so also the imposed loads will be of transient nature. Instead, a simplified wave-on-deck model was adopted, where shallow-water flow is assumed on top of the pontoon. The pontoon was divided into several strips, and the relative wave elevation above the pontoon's deck level was extracted in the centre of each strip. In doing so, the incident wave elevation was multiplied with an amplification factor to account for wave non-linearity and local diffraction effects. If at a given time step the relative wave elevation is so that the wave exceeds the freeboard, a vertical force is computed for the strip; otherwise, the vertical force is zero. The vertical forces on all strips are accumulated to a vertical force and a roll moment that are imposed as external loads in the pontoon's equations of motion. Hence, the model, although simplified, is physics based and can reflect the transient type of loading. The wave amplification factors are deliberately chosen somewhat on the conservative side.

To investigate the effects of freeboard exceedance on the global bridge response, studies on a single pontoon were first conducted in a 100 year and 10000 year sea state with and without wave spreading, respectively. The model was also implemented in a global OrcaFlex analysis for a 100 year sea state and an exaggerated 10000 year sea state, respectively.

3.6.3. Findings and recommendations

For the single-pontoon model, freeboard-exceedance events were observed in the 100 year sea state with moderate influence on the heave and roll motions. In general, freeboard exceedance may lead to both reduced motion (damping) and amplified motion (excitation). This is largely governed by the length of the force impulse divided by the relevant natural period. In the 10000 year sea state, significant amplification of the heave motions was observed, while the roll motion was unaffected or slightly reduced. When incorporated in the global model, freeboard exceedance was found to have negligible influence on strong and weak axis bending moments in the 100 year sea state while leading to a slight increase in the exaggerated 10000 year sea state. The analyses performed with the proposed model here indicates that 1) freeboard exceedance may occur in 100 and 10000 year sea states, but 2) has un-dramatic consequences for the global bridge response. However, the effect of including the model for all pontoons simultaneously has not been investigated. This should be done in future phases of the project in order to investigate correlation effects. In addition, a larger number of sea states should be considered. The proposed freeboard model should be validated and possibly calibrated against CFD analysis and/or dedicated model tests. CFD analysis or model test should also be used to investigate the relationship between wave-current interaction effects and freeboard exceedance. If the model proposed in the present phase is found to be inaccurate, there are more refined models available where the flow on deck of the pontoon is resolved in space and time through solving the shallow water equations. Such method could be considered, although it is expected to substantially increase the computational time in a global response analysis.

4. Analysis, Modelling and Response

4.1. Mooring line damping

4.1.1. Problem description

The mooring lines contribute significantly to the global damping for many of the deformation modes of the bridge. This large effect was not properly documented in Phase 3 of the project and raised as an uncertainty at the beginning of Phase 5.

4.1.2. Performed investigation

Several types of investigations were performed in the work to better understand the global effect of mooring line response:

- The methodology and input coefficients used for mooring line damping was checked, and found to be aligned with conventional offshore practise.
- A preliminary sensitivity study was conducted in which the effect of pretension, drag coefficients etc. was investigated on a mooring cluster, ref. [9]
- An analytical approach to mooring line damping based a quasi-static considerations was developed, in which a nonlinear mooring cluster damping characteristic was extracted, ref. [10]. The findings compare well with findings from the offshore industry. The local dynamic line response is small compared to the quasi-static contribution from lateral motion of the pontoon.
- Decay testing was performed on the global model in orcaflex in which the mooring lines were included with the relevant viscous drag coefficients. The bridge was deformed into mode shapes based on an eigenmode analysis and released, and the corresponding modal damping level was found. Results with and without mooring were compared, and the moorings were found to be a significant source of modal damping for the modes in which significant pontoon motions was present. See Appendix F [11] for more details.
- The effect of global bridge deformations due to transverse loads, temperature and tide affects the mooring line pretension, but the effect on global modal damping is limited and within acceptable limits.

4.1.3. Findings and recommendations

With the performed investigations the uncertainty with the global effect of mooring line damping is removed. The physics behind the damping is now documented and found in agreement with published results from the offshore industry.

4.2. Simulation time, ramp-up and time step

4.2.1. Problem description

The simulation time was highlighted as a challenge from Phase 3 of the project, in which 1-hour simulations with a 300 second ramp-up was used. Convergence of dynamic response and transient effects due to rapid startup was of concern. This is especially a concern for structures with long eigen periods such as the K11 concept (108 s), whereas the moored concepts such as the preferred K12 has half the period (56 s for K12 with the proposed mooring configuration).

4.2.2. Performed investigation

A sensitivity study was conducted to investigate the response of the K12 concept, in which a single seed of wind sea, swell and wind was simulated for 3, 3 and 6 hours respectively. The three simulations trigger different eigenmodes and may as such have different convergence rates.

A rolling mean and standard deviation were used to assess the convergence, both decreasing with larger statistical windows. The statistical variation will therefore typically be smaller between several longer simulations, and higher between several shorter simulations. Therefore, it may be necessary to simulate more seeds if the duration is short.

The rolling mean and standard deviation are stationary processes, meaning that the dynamic processes in the simulation are stable even at the very beginning of the simulation. A simulation of 3600 seconds is therefore long enough to meet a stable condition and to keep statistical variation between seeds to a low level.

The effect of duration of the ramp-up stage was studied separately using wind sea and swell waves. Very short ramp-up stages (100 s) had some transient effects, but these were not present for simulations with 300 s ramp-up.

The effect of varying time step from 0.1 to 0.5 s was investigated for a wind sea condition, in which more of the shorter eigen modes of the bridge is excited. A time step of 0.2 s was found to be sufficient to capture the response.

4.2.3. Findings and recommendations

Based on the sensitivity study it was confirmed that 300 seconds ramp-up, 1-hour duration of the simulations and 0.2 s time steps were enough to give a stable response with low statistical variance between seeds and negligible transient effects due to ramp-up.

4.3. Spectrum discretization

4.3.1. Problem description

The wave spectrum is discretized into a set of discrete wave components which are simulated in time domain. Whether a structural eigenmode is excited or not depends on the frequencies of the wave components present in the simulation. The magnitude of the structural response depends on the wave energy (amplitude) present in the wave components. It is therefore important to discretize the wave spectrum into enough wave components close to the important structural eigenmodes to avoid unrealistic responses. To keep the calculation time to a minimum the total number of wave components should be kept to a minimum.

4.3.2. Performed investigation

In OrcaFlex, the wave spectrum may be discretized using three different approaches:

- Arithmetic progression (constant frequency increments with varying wave amplitude)
- Geometric progression (constant ratio between successive frequencies with varying wave amplitude)
- Equal energy (constant wave amplitude with varying frequency increments)

Arithmetic progression requires a high number of wave components to avoid signal repetition and should therefore not be used to discretize a wave spectrum in OrcaFlex as the calculation time will increase drastically.

The wave discretization was studied by applying the equal energy approach with 150 to 750 wave components in 10 seeds of 3600 s. In the equal energy approach, the frequency increments between wave components are inversely proportional to the wave spectrum energy. If little wave energy is present near important structural modes, the response may therefore be unrealistic due to few wave components. To refine the discretization near these frequencies the total number of wave components may have to be increased quite a lot.

A refined discretization method was also developed to improve the shortcomings of the equal energy approach. In this method, a frequency increment distribution is used to ensure enough wave components where they are needed.

4.3.3. Findings and recommendations

It was found that approximately 600 components were enough to achieve convergence for the important forces and moments. It is thus confirmed that the wave spectrum discretization used in the global analysis are converged.

Using the refined discretization method, the number of wave components may be reduced to about 150 components without compromising the precision of the results. The calculation time could therefore be decreased substantially by applying the refined discretization method.

4.4. Shear stiffness

4.4.1. Problem description

The beam element in Orcaflex does not account for shear stiffness, which may be relevant for certain weak-axis modes. Simplified investigations were performed in the previous phases of the project to assess the effect, and it was found to be of minor importance, but the uncertainty was not closed.

The effective shear areas of the bridge girder in the vertical direction are low, and accounting for shear deformation may as such reduce the stiffness of the girder which again increase the modal periods. Shear deformation may also be relevant in the strong axis in which the width of the cross-section is 4-5 times the span length of the girder between pontoons. However, environmental loads will not trigger the strong-axis deformation to a notable extent.

4.4.2. Performed investigation

Simulations with and without shear stiffness were conducted in RM-bridge in which this can be selected as an option in the element formulation, see [12] for details. Two types of simulations were conducted; eigen mode calculation and a time-domain response assessment with wind loading.

The eigenmode calculations show a shift in the period of the vertical piston modes (every other pontoon up or down) of around 5%, whereas quasi-static assessment of the same mode yields a change of around 8 %. The modal period is between 2-3 seconds, in which there is significant wave loading for all modes. Hence, the shift in eigen period due to shear stiffness will not affect if the piston mode is excited in wind sea conditions (e.g., the mode in which every other pontoon goes up or down causing large weak-axis moments).

The wind response assessment revealed a shift in the response around 3 seconds (as for the eigen period) and around 1 seconds. The latter is a vibrational mode of the bridge girder that is not excited by environmental loads to an extent at which it is governing for design.

4.4.3. Findings and recommendations

The investigation revealed a 5-10% difference in weak-axis piston eigen mode, and some change in the lower period vibrational modes internally in the bridge girder. This does not lead to a significant change in response, and the lack of shear stiffness in Orcaflex is as such considered not to be a concern for the global response of the bridge.

4.5. Coupled vs. uncoupled response

4.5.1. Problem description

The main design method in previous phases has assumed uncoupled environmental conditions (such as wind sea, swell and wind), and verified this with a limited amount of simulations with coupled environmental conditions. For linear processes with linear response decoupling is a valid assumption. However, mooring line response is nonlinear so that e.g. temperature and tide change the linear stiffness of the system due to the change in static pontoon position.

The response of the bridge is a complex process, and the “true” response is coupled. However, this requires accurate input data with fully correlated data for all environmental contributions and a vast amount of simulations in order to be the only design method.

4.5.2. Performed investigation

It was decided to maintain the uncoupled approach as the main design method, but the checks with the coupled approach was more elaborate than in previous phases. The same environmental conditions were investigated using a coupled and decoupled approach. The effect of temperature and tide was checked with separate coupled simulations. Ten seeds were used for each condition, and the AUR method was used to estimate the 90-percentile response. This was compared to the expected maximum found using the decoupled approach.

For axial force, the coupled approach was found to yield somewhat higher response. However, weak- and strong-axis bending moment was reduced in the coupled simulations. Especially swell caused large differences, in which the decoupled approach gave a pure excitation of a mode that was not seen when coupled with wind and wind sea. This is likely due to a combination of aerodynamic damping and disturbance from the wind sea that is not captured for the decoupled approach.

The resulting stresses were for all points considered worse for the decoupled approach, and the design of the bridge was thus based on a safe set of response data.

4.5.3. Findings and recommendations

With the performed investigation, the decoupled approach was found to yield conservative results for design of the bridge girder. Mooring lines were designed according to the coupled approach.

The assumption of decoupled response was thus confirmed as a reasonable design choice that significantly improves the complexity and amount of simulations needed to include the relevant effects in a rational manner.

4.6. Extreme value estimation of stresses

4.6.1. Problem description

Stresses due to environmental loads are typically non-Gaussian processes, and the extreme values cannot be found from a single simulated time-series using a peak factor. Instead, several realizations of the time series must be simulated using different seeds, and extreme values can then be estimated. Typically, the Gumbel method is applied using the max value from each realization. Thus, only one data point is obtained from each realization, and the simulation length must be exactly one hour if the 1-hour max is to be estimated.

4.6.2. Performed investigation

As an alternative to the Gumbel method, the average upcrossing rate (AUR) method for estimating short-term extreme response has been implemented. The method is described in the memo [12]. The AUR method can be applied to both Gaussian and non-Gaussian response processes, and does not require a specific simulation time. Compared to the Gumbel method for extreme response, the AUR method utilizes more of the data in the simulated time series, and is thereby expected to be more accurate.

4.6.3. Findings and recommendations

With the implementation of the AUR-method, a more flexible and accurate method is available for the estimation of short-term extreme values.

4.7. Characteristic response vs. characteristic load

4.7.1. Problem description

The 100-year response is defined as the response value that is exceeded in average once every 100 years. Ideally, the 100-year response should be calculated from a full long-term extreme response analysis, taking into account all possible sea states. However, due to the large computational cost, the 100-year response is commonly estimated in a simplified manner by considering only 100-year sea states. If each sea state is specified in terms of only one parameter, e.g. significant wave height Hs, the 100-year sea state is simply defined by the Hs-value that is exceeded in average once every 100-years. However, if the sea states are specified by two parameters, e.g. Hs and Tp (peak period), there is no longer a unique way of the 100-year sea states. Still, environmental contours (curves in the Hs-Tp space) can be established which are expected to give rise to the 100-year response. If wave direction is included in addition to Hs and Tp, directional contours can be established, but in this case the definitions vary even more.

The assumption that the 100-year sea states give rise to the 100-year response is a simplification that must be validated by more accurate methods of calculating the 100-year response.

4.7.2. Performed investigation

Recently, methods have been developed which provide more accurate estimates of the 100-year response at a significantly reduced computational cost [1, 2]. These methods are referred to as inverse reliability methods. An inverse reliability method has been implemented and the 100-year response was estimated for 20 different responses of the concept K12_07 using this method. The results were compared with the 100-year responses estimated from the 100-year sea states.

4.7.3. Findings and recommendations

The 100-year responses estimated from the 100-year sea states gave roughly similar values as the 100-year response estimated directly using the inverse reliability method. However, in some cases using the inverse reliability method gave a 100-year response more than 100 % larger. This indicates that estimating the 100-year response from the 100-year sea states might be too rough in some cases. It is recommended that further studies are carried out for the estimation of 100-year response. More investigations using inverse reliability methods can be performed, but a full long-term extreme response analysis will also be necessary for comparison.

4.8. Dynamic Effects of Traffic on the Bridge

4.8.1. Problem description

Traffic affects the dynamic response of the bridge in a few ways;

- The weight of the traffic may affect the natural frequencies and mode shapes
- Wind loads increase due to change in aeordynamic coefficients and exposed area towards the wind
- Dynamic effects of the moving traffic weight may cause direct dynamic response in the bridge (mostly important for fatigue as long as the bridge is not used for trains)

Of these, the two first were investigated for global response, and the third only for local fatigue response.

4.8.2. Performed investigation

A version of the K12 bridge model was modified to include both increased mass (assumed as 2 tons/m) and increased aerodynamic coefficients to account for the wind effects. Further, the hydrodynamic behaviour was adjusted reflect the increased draught of about 30 cm due to the traffic load. The model was simulated with 1-year environmental conditions and then compared to an empty bridge model with same environmental loads. The study was documented in Appendix G, [13].

The mode shapes of the bridge were not significantly affected by the traffic load, but the periods increased up to two seconds (varying between the modes). The change in modal periods will not move modes into the wave-excited regime, rather move modes away.

The increased hydrodynamic loading due to increased draught of the pontoon did not seem to affect the bridge response.

The static vertical bridge response (shear and weak-axis moment) increased due to the presence of traffic, but the ULS2 traffic load scenario remained governing. The transverse response of the bridge increased somewhat due to the increased aerodynamic loading, but the strong-axis bending moment is still significantly less than the ULS3 response in which 100-year wind on empty bridge is considered.

4.8.3. Findings and recommendations

The investigation has shown that the presence of traffic affects the bridge response somewhat, but the changes are not governing for the design.

Further studies are not required in terms of a feasibility of the concept, but it is recommended to include this as a sensitivity check during detailed design to ensure that all possible load scenarios are evaluated properly.

4.9. Imperfections

4.9.1. Problem description

Imperfections from fabrication, both local and global, will be present in the bridge once installed. The imperfections can have a global consequence (by reducing the global buckling capacity of the bridge) and a local effect (by reducing the local buckling capacity of the cross-section). An imperfection may within certain limits force a response into a certain mode.

4.9.2. Performed investigation

No investigations on imperfections were conducted for the global behavior of the bridge, as the mooring system contributes significantly to the global buckling capacity of the bridge. This should however be accounted for if the K11 bridge was chosen.

The local imperfections causing a reduced local plate buckling capacity was only accounted for when investigating the plastic torsional capacity of the column when subject to ship collisions, for which it was found to not be sensitive.

Local imperfections on the bridge girder causing a reduced plastic capacity of the cross section was not addressed. For elastic response within the ULS requirements the local buckling check inherently accounts for imperfections.

For fatigue, local imperfections are directly included as fabrication tolerances on the stress concentration factors.

4.9.3. Findings and recommendations

It is recommended for study the plastic capacity of the bridge cross-section during detailed design in which all imperfections are accounted for. Further, a sensitivity check of global imperfections should be performed, but this is not considered to be a cause of concern with respect to the global response on the bridge.

4.10. Comfort evaluation

4.10.1. Problem description

During phase 3 of the project the accelerations of the bridge girder were considered as high, and it was not sure if the root-mean-square acceleration criterion that was used gave meaningful limits of bridge comfort. A more detailed investigation was required during phase 5, and a new overall vibration total value (OVTV) criterion was proposed in the design basis.

4.10.2. Performed investigation

A dynamic model of a vehicle was established based on input from NPRA. The dynamic behavior of the bridge girder due to environmental loads was investigated in detail for all the bridge concepts, and combined with the quasi-static deflection due to the weight of passing traffic.

The dynamic vehicle model was used to assess the vehicle response for both bridge motion and the local motion of the vehicle when subject to local wind loads. The calculated accelerations in the driver's seat in the vehicle model was used as a basis to evaluate the OVTV model.

The findings indicate that the bridge girder motion utilized about 1/3 of the OVTV criterion. However, local wind on the vehicle overutilized the criterion with a factor of 3. The bridge was thus assessed as *fairly uncomfortable* rather than the required *not uncomfortable*. No large differences were observed between the concepts.

4.10.3. Findings and recommendations

Using the OVTV criterion as a basis to perform design development based on the driving comfort is likely an immature approach, and NPRA currently has an academic study underway to define a suitable criterion. Based on the findings during this phase of the project the bridge motion was not a large contributor to the discomfort. Hence, it is deemed fairly uncomfortable to drive in a 1-year storm with the turbulence intensities at the bridge location irrespective of the bridge motion.

It is noted that the wave conditions given in the metocean design basis for phase 5 of the project is considerably less than those given for phase 3, resulting in nearly a 50% reduction in dynamic bridge motion. However, it is not possible to conclude that the absolute level of comfort when using the bridge is at an acceptable level based on the proposed bridge concept and the phase 5 wave conditions. Further work on this is recommended, and a better acceptance criterion for driving comfort would be much appreciated.

4.11. Fatigue assessment

4.11.1. Problem description

A full assessment of the fatigue capacity of the bridge is challenging due to the extent of the structure, the complexity of the dynamic behavior and the behavior of local details subjected to both local and global loads. Hence, the fatigue estimate from previous phases had a large uncertainty.

4.11.2. Performed investigation

Several improvements in the methodology have been achieved during Phase 5 of the project:

- The local and global deformation of the bridge is now accounted for for traffic loads, combining the global influence lines with the local tire pressure history to create a local stress-time event in each considered detail.
- A stochastic traffic pattern is defined with traffic in both directions in all lanes, capturing the global and local effect of overtaking vehicles and oncoming traffic.
- Uncoupled and coupled simulation of environmental loads were compared and small differences were found.

The new approach has led to reinforcements of the bridge girder, primarily the top deck plate thickness and the trapezoidal stiffeners in the slow traffic lanes. Further, requirements are developed for placements of longitudinal and transverse welds in plates and stiffeners.

4.11.3. Findings and recommendations

The new approach has considerably reduced the uncertainty related to the methodology of the fatigue assessment for flexible floating bridges.

Some uncertainties remain:

- Coupled global and local response of e.g. the interface between bridge girder and column
- Some local structural optimization is required to achieve sufficient fatigue life
- A traffic load model should be developed based on actual traffic data at the bridge location (a FLM5 model)
- Wave interaction effects and inhomogeneous sea states may affect the fatigue capacity.

4.12. Ship collisions

4.12.1. Problem description

Bridge crossings are inherently exposed to collision risk, and the Bjørnafjorden bridge both has significant traffic along the bridge due to its proximity to a major shipping lane and some traffic crossing the bridge due to activities inside of the bridge location. There is significant uncertainty in the estimation of relevant design scenarios to consider, but this is outside of the scope of the AMC group during the project phase.

Further uncertainty is found in the local and global response to a ship impact event; locally how the structures interact and how large forces over how long time that are transmitted to the bridge system, and globally how the bridge responds to such loads and where energy is dissipated.

4.12.2. Performed investigation

The local ship collision response was studies decoupled from the global response, and the assumptions behind this is not strictly valid for the collision durations that were simulated. However, the local methodology itself is of high accuracy, using the best available and most thoroughly verified methodology. The main uncertainty is thus on the selected scenario; impacting vessel type, size, velocity and impact location. Several variations were simulated to mitigate this uncertainty, and the ones considered most unfavorable was used for local and global capacity evaluations.

Significant improvements were achieved on the global collision methodology as opposed to the previous project phases; the local energy dissipation in the collision was not accounted for and the total energy balance was maintained to a much higher level. A wide range of scenarios were simulated to cover possible scenario variations. The global response evaluations as such have a considerable reduction in uncertainty.

Ship collisions were found to be dimensioning for parts of the high bridge and the northern abutment, several of the anchors as well as for the columns connecting the pontoons to the bridge girder. A large uncertainty in the latter is the range of impact angles and associated impact energies that are realistically possible to achieve. Coupled local and global deformation was considered in order to properly study the response. With worst-case assumptions it is possible (but somewhat costly) to get a reasonable design of the columns.

4.12.3. Findings and recommendations

Overall the bridge was found robust to ship collision events. The ship collision scenarios are expected to be reduced considerably in the next project phase due to a re-routing of the navigational channel for ships passing along the bridge, further improving the robustness against ship collisions.

It is recommended to continue the study of ship collision response of the bridge during the next project phase, with emphasis on the response of the columns locally and the high bridge and northern abutment globally. The plastic capacity of the bridge girder should be assessed, and its behavior included in the global model to possible consequences. Coupled simulations with local and global response should be extended to include more structural components and scenarios.

4.13. Effect of skew wind

4.13.1. Problem description

Conventionally, wind loading to bridges has been applied based on a decomposition of the wind field velocities in the direction transverse to and along the bridge girder, for which transverse wind generate drag, lift and overturning moments whereas longitudinal wind generate frictional loading. This method was adopted for global simulations herein (neglecting the frictional component)

The alternative approach is to calculate the drag, lift and moments directly in the wind direction, thereby evaluating the actual cross-section of the bridge as seen by the wind with its instantaneous wind coefficients. The angle in the horizontal plane between the wind direction and the bridge transverse axis is herein termed *yaw* angle.

For straight bridges the wind load response will normally be highest for winds transverse to the bridge, and decomposition of the wind field is thus a reasonable approach. For large bridges with curvature in the horizontal plane (such as the preferred K12 concept over Bjørnafjorden) it is more difficult to select a governing wind direction due to the possible effect of skew wind.

4.13.2. Performed investigation

A screening study was performed with varying wind direction based on the conventional approach with wind decomposition in the bridge axis. Winds coming transverse to the line between the Northern and Southern abutment was found to yield highest responses in the bridge girder and selected for design.

The wind load model used in Orcaflex was modified to include the possibility of skew wind by interpolating on a set of wind load coefficients based on the *skew* angle (the method considers all six degrees of freedom between the instantaneous wind direction and instantaneous bridge position and orientation).

A simplified 2D CFD study was conducted to obtain aerodynamic coefficients with varying wind direction relative to the bridge girder. The 2D approach has limitations for larger skew angles, and a full 3D CFD and/or model tests are recommended for future verification.

Based on the skew wind load model a screening of bridge response to various wind directions was performed and compared to the same screening with wind decomposition. The strong-axis moment was highest for wind transverse to the main bridge axis both with and without the skew wind effect. However, with increasing skew angles the bending moment was reduced when not considering skew effects but maintains a similar amplitude if the effect is included. The axial load increased significantly with increasing skew angle when considering the skew effect.

4.13.3. Findings and recommendations

The assessment of skew wind is at a low maturity stage and should be better understood before drawing any conclusions as to the response of the bridge. The aerodynamic coefficients should be evaluated in 3D CFD and compared with model tests. The skew wind effect should be assessed with varying length and radius of curvature of the bridge span to understand when and if the skew effect is important.

It is recommended to continue this study towards the detailed design of the project.

5. Parametric excitation

To evaluate parametric excitation the following procedure was applied:

- Global response analysis of the defined swell, windsea and wind conditions to determine dynamic axial force response (σ_N).
- Evaluate the critical axial force response for each uncoupled eigenmode and each critical frequency ratio considering the geometric stiffness variation and damping of each mode (A_{cr}).
- Evaluate the *onset criterion* defined by NTNU/NPRA in the provided background material, i.e., ensure that $\sigma_N/0.4 < A_{cr}$.
- If the concept fails the onset criterion, the stochastic axial force variation is approximated conservatively as harmonic and the corresponding *terminal* response (a term chosen deliberately to indicate that the response is only reached in an asymptotic manner) is estimated. The response converges towards this asymptotic level due to the presence of quadratic drag damping. For the determinaltion of the terminal response, the response level is based on a probability of exceedance of 0.01% and 10% for the 100-year and 10000-year conditions, respectively.
- Repeat the estimation of the terminal response level including an 20% increase of axial force amplitude and 20% decrease in quadratic damping, to assess the robustness towards uncertainties.

Furthermore, the results were verified by conduction Monte Carlo simulations on the single-degree-of-freedom (SDOF) system, i.e., the system modes, based on the obtained spectral density of the axial force amplitude.

For a detailed description of the procedure and an evaluation of the uncertainties involved, please refer to Appendix S [14].

5.1. Modelling parametric excitation

5.1.1. Problem description

To model parametric excitation, the system modes were utilized. This approach involved two apparent simplifications:

- The system matrices were assumed to be diagonal, i.e., the system modes were independent, to enable SDOF predictions.
- The system was assumed to behave linear. Even though parametric excitation is considered a highly nonlinear phenomenon, using a linearized modal geometric stiffness the linear approach was able to represent the effect.

All assessments were conducted in a self-developed Python framework. This represents an important potential source of errors, and self-checks and verification studies are considered crucial.

5.1.2. Performed investigation

To gain faith in the linearized SDOF approach, comparison to the results obtained from a full Orcaflex global analysis model was conducted. Furthermore, the diagonality and complexity of the full modal system was evaluated, to assess the validity of the diagonal approach.

To verify the validity of the time simulations used to verify the terminal response assessment, simulations with axial force slightly below and above the critical amplitude were conducted to ensure that the set-up could correctly identify the critical amplitude. Furthermore, the predicted terminal response level from multiple harmonic scenarios were compared to the simulated response.

5.1.3. Findings and recommendations

The comparison between the linearized model and the full Orcaflex global analysis model, shown in Appendix S [14], indicate that the simplified approach yields conservative results. The assessments of complexity and diagonality indicate that the first low damped system modes (1–10) are behaving almost completely diagonal.

The critical amplitude and the terminal levels estimated for harmonic axial force variation are in perfect agreement with the simulated SDOF results.

5.2. Parameters for evaluation of parametric excitation

5.2.1. Problem description

Uncertainty in all modal parameters could affect the resulting response. The most uncertain parameters are the following:

- Applied axial force ampltiude, N
- Quadratic damping coefficient, c_{quad}
- Linear damping, represented by the critical damping ratio, ξ
- Geometric stiffness normalized with respect to axial force, $\hat{k}_g$

Additional uncertainties are involved in the estimate of the geometric stiffness, as this is established through a self-developed Python code. Furthermore, the geometric stiffness is based on the fact that all axial force amplitude is applied constant along the entire girder for all modes considered.

5.2.2. Performed investigation

To assess the effect of uncertainties of the most crucial parameters, their implications on the estimated terminal response were evaluated. Small changes in frequency might lead to larger effects on the total damping level, due to the frequency-dependent damping contributions, even though the frequency-dependent damping contribution itself might be considered relatively certain (potential damping is the most obvious example). As a verification on the geometric stiffness, a separate analysis was conducted in RM Bridge for K11, for comparison with the results from the self-developed code.

5.2.3. Findings and recommendations

As the linear damping is almost merely comprised of the structural damping for the modes of interest (0.5% of critical damping), it is considered relatively certain, at least expected to be on the conservative side. The effect of uncertain axial force amplitude could be relatively large because it is zero for values below the critical amplitude but could yield large response values for amplitudes slightly above. An uncertain quadratic damping coefficient affects the response in a very large degree for lower values, as the response tends to infinity when the it approaches zero (see Figure 5-1). Furthermore, lower quadratic drag damping exaggerates the implications of uncertainty from all other parameters involved. Note that uncertainties included in this parameter typically would represent inherent uncertainties from, e.g., the damping coefficient C_d.

Comparison of geometric stiffness obtained from RM Bridge matches reasonably well with the value obtained directly (see [14]).

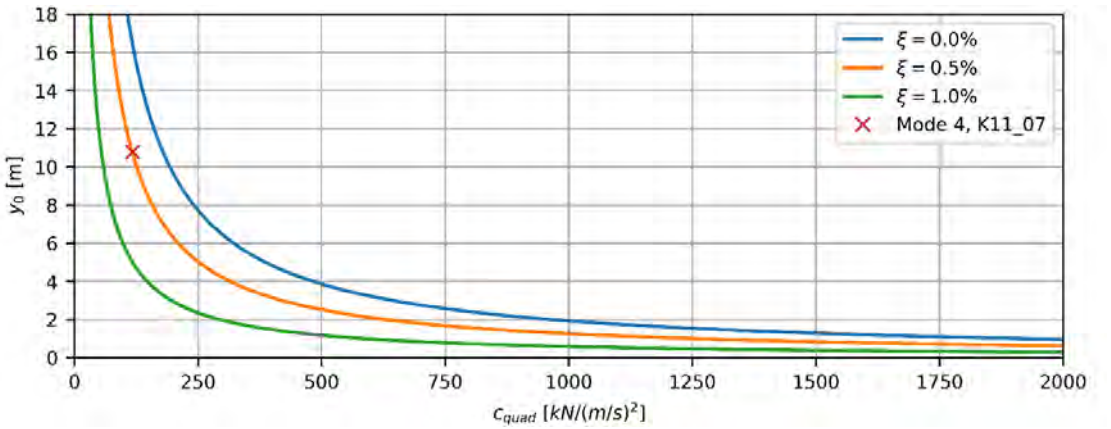

Figure 5-1. Effect of quadratic damping on the terminal level for mode 4 on K11, exposed to axial force variation with circular frequency $2\omega_d$.

6. References

[1] F.-I. G. Giske, "Long-Term Extreme Response Analysis of Marine Structures Using Inverse Reliability Methods," Norwegian University of Science and Technology (NTNU), Trondheim, 2017.

[2] F.-I. G. Giske, K.-A. Kvåle, B. J. Leira and O. Øiseth, "Long-term extreme response analysis of a long-span pontoon bridge," *Marine Structures,* vol. 58, pp. 154-171, 2018.

[3] AMC, "10205546-11-NOT-193 Long-term wave response, rev. 0," 15.08.2019.

[4] E. Vanem, "A comparison study on the estimation of extreme structural response from different environmental contour methods," *Marine Structures,* vol. 56, pp. 137-162, 2017.

[5] W. Chai and B. J. Leira, "Environmental contours based on inverse SORM," *Marine Structures,* vol. 60, pp. 34-51, 2018.

[6] E. Ross, O. C. Astrup, E. Bitner-Gregersen, N. Bunn, G. Feld, B. Gouldby, A. Huseby, Y. Liu, D. Randell, E. Vanem and P. Jonathan, "On environmental contours for marine and coastal design," in *Proceedings of the ASME 2019 38th International Conference on Ocean, Offshore and Arctic Engineering (OMAE 2019)*, Glasgow, 2019.

[7] G. Feld, P. Jonathan and D. Randell, "On the estimation and application of directional design criteria," in *Proceedings of the ASME 2019 38th International Conference on Ocean, Offshore and Arctic Engineering (OMAE 2019)*, Glasgow, 2019.

[8] AMC, "SBJ-33-C5-AMC-21-RE-108 : Appendix H: Global Analyses - Special studies Rev. 0," 15-08-2019.

[9] AMC, "10205546-12-NOT-065 Moorling line damping, rev. 0," 18.02.2019.

[10] AMC, "10205546-11-NOT-095 Rev1. Analytical mooring line damping," 2019.

[11] AMC, "SBJ-33-C5-AMC-90-RE-106 : Appendix F: Global Analyses - Modelling and assumptions Rev. 0," 15-08-2019.

[12] AMC, "10205546-11-NOT-059 Estimation of extreme response using the AUR method, rev. 0," 29.03.2019.

[13] AMC, "SBJ-33-C5-AMC-90-RE-107 : Appendix G: Global Analyses - Response Rev. 0," 15-08-2019.

[14] AMC, "SBJ-33-C5-AMC-90-RE-119 : Appendix S: Parametric excitation Rev. 0," 15-08-2019.

[15] AMC, "SBJ-33-C5-AMC-20-RE-105 : Appendix E: Aerodynamics Rev. 0," 15-08-2019.

[16] AMC, "SBJ-33-C5-AMC-22-RE-109 : Appendix I: Fatigue analyses Rev. 0," 15-08-2019.

[17] AMC, "SBJ-33-C5-AMC-27-RE-110 : Appendix J: Ship collision Rev. 0," 15-08-2019.

[18] AMC, "SBJ-33-C5-AMC-26-RE-113 : Appendix M: Anchor systems Rev. 0," 15-08-2019.

Concept development, floating bridge E39 Bjørnafjorden

Appendix G – Enclosure 17

Static results K12_07

Static Results K12_07

August 9, 2019

Contents

1 Current loads

1.1 Axial force

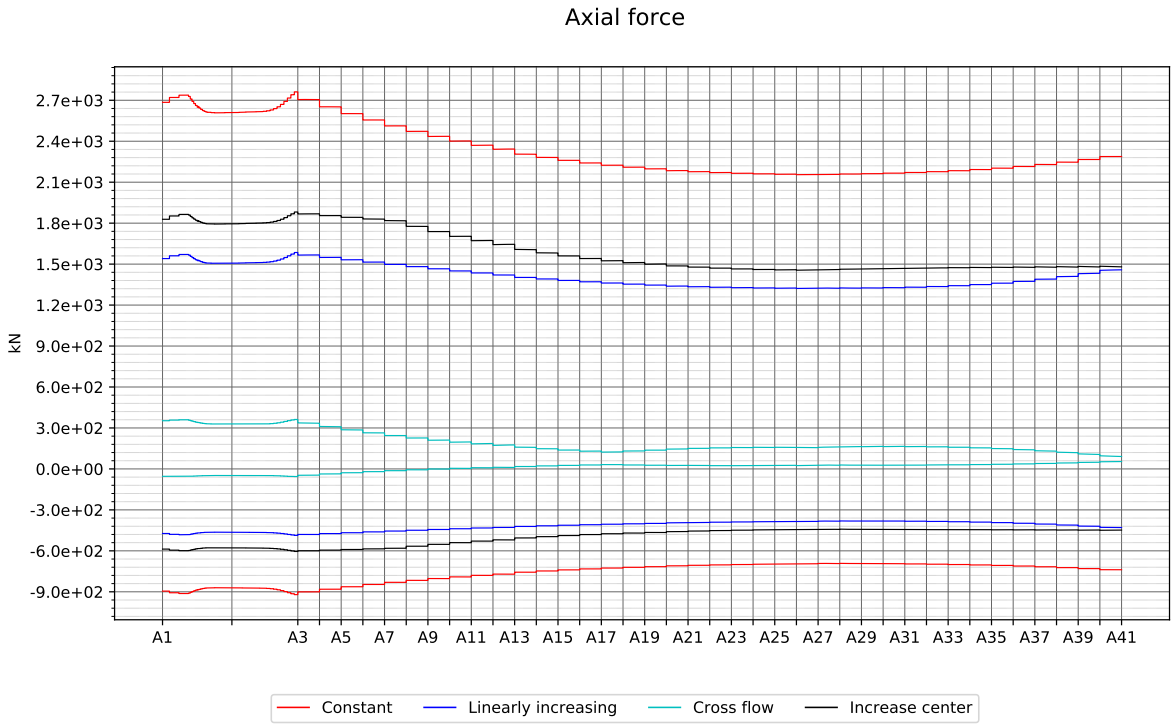

1.2 Bending moment about strong axis

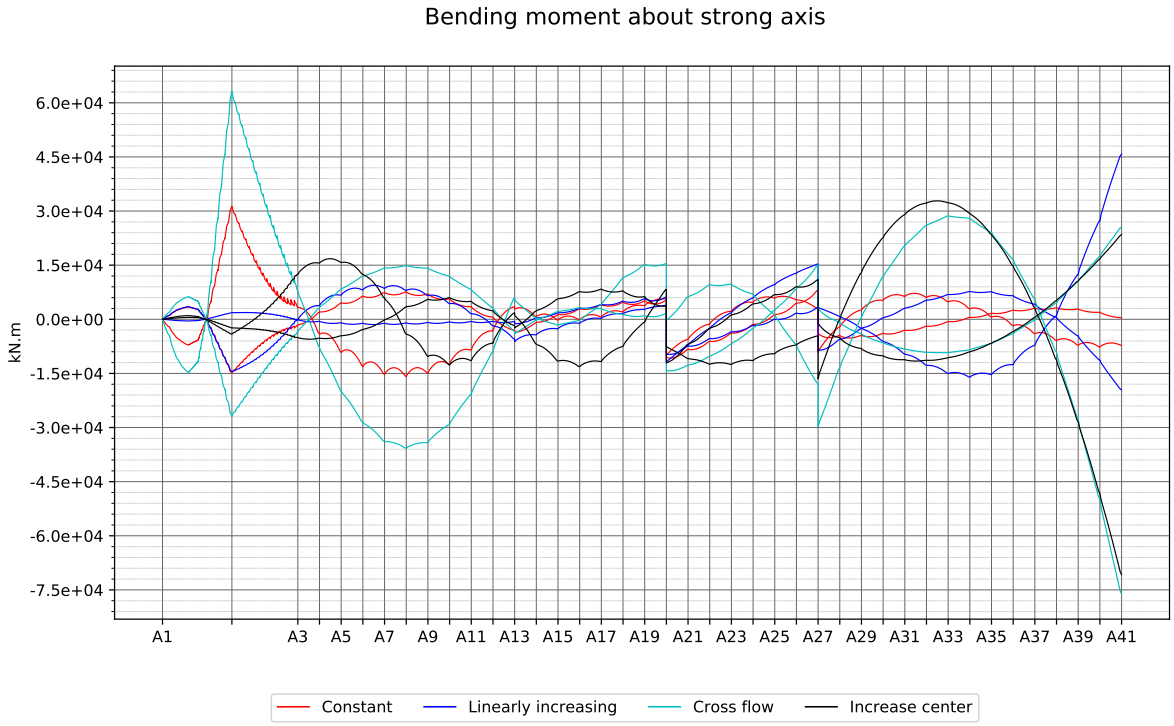

1.3 Bending moment about weak axis

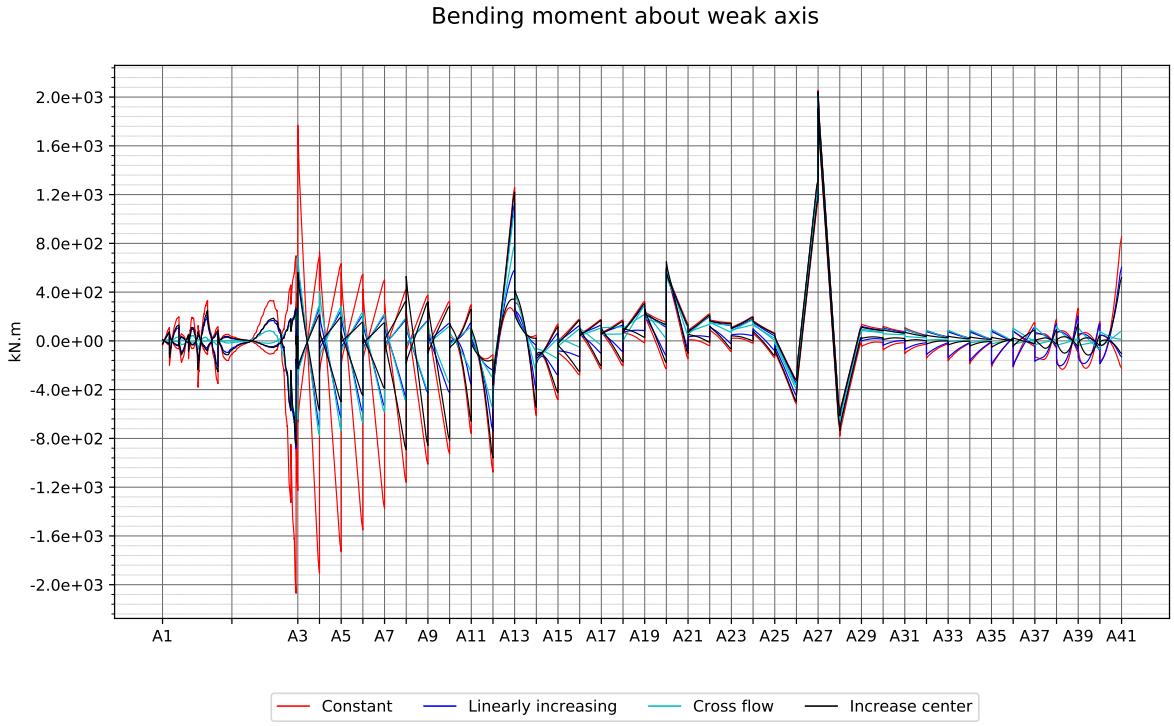

1.4 Torsional moment

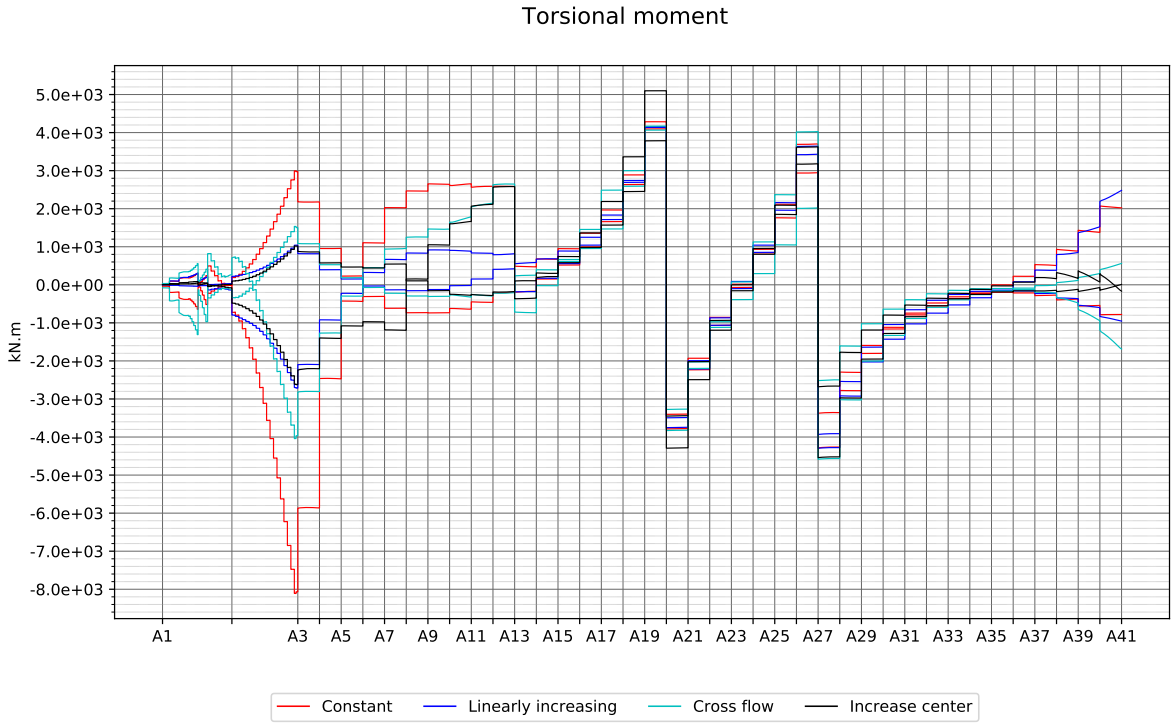

1.5 Vertical shear force

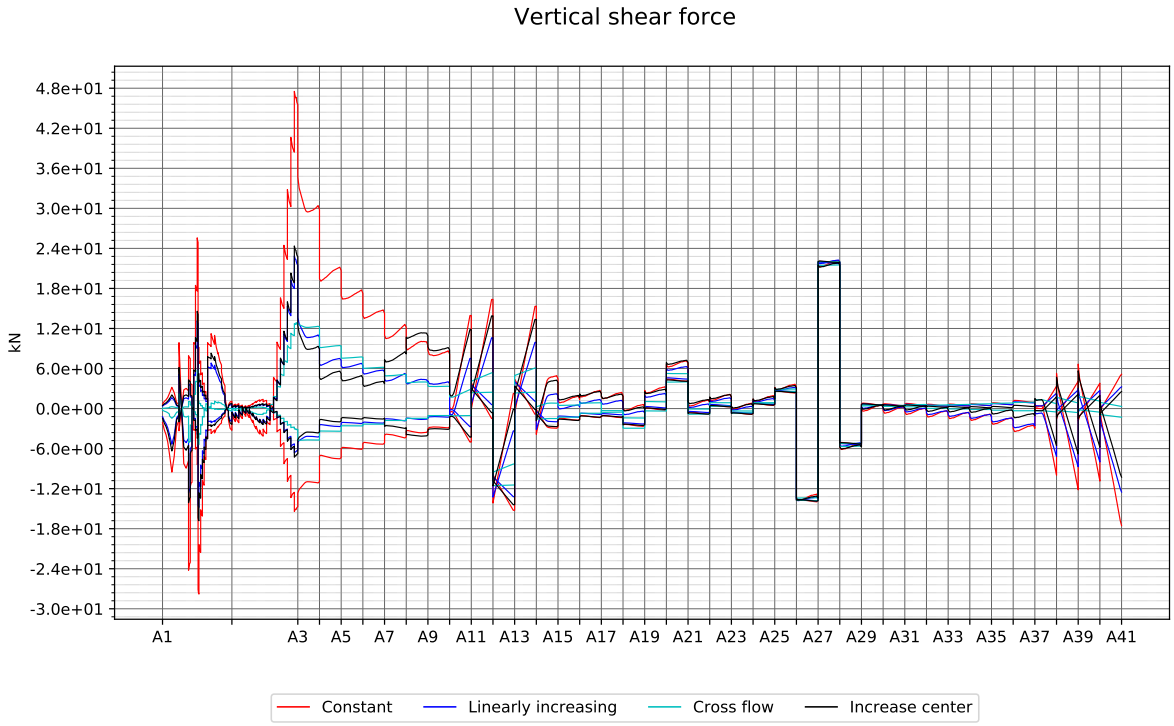

1.6 Transverse shear force

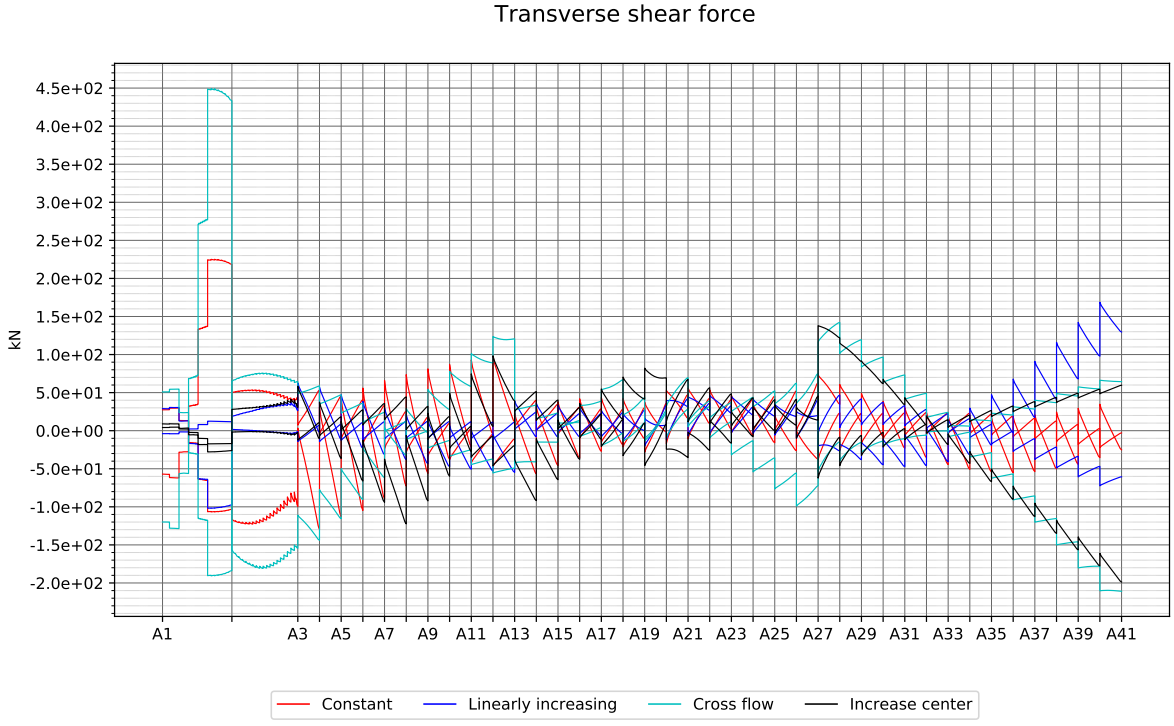

1.7 Global Longitudinal displacement

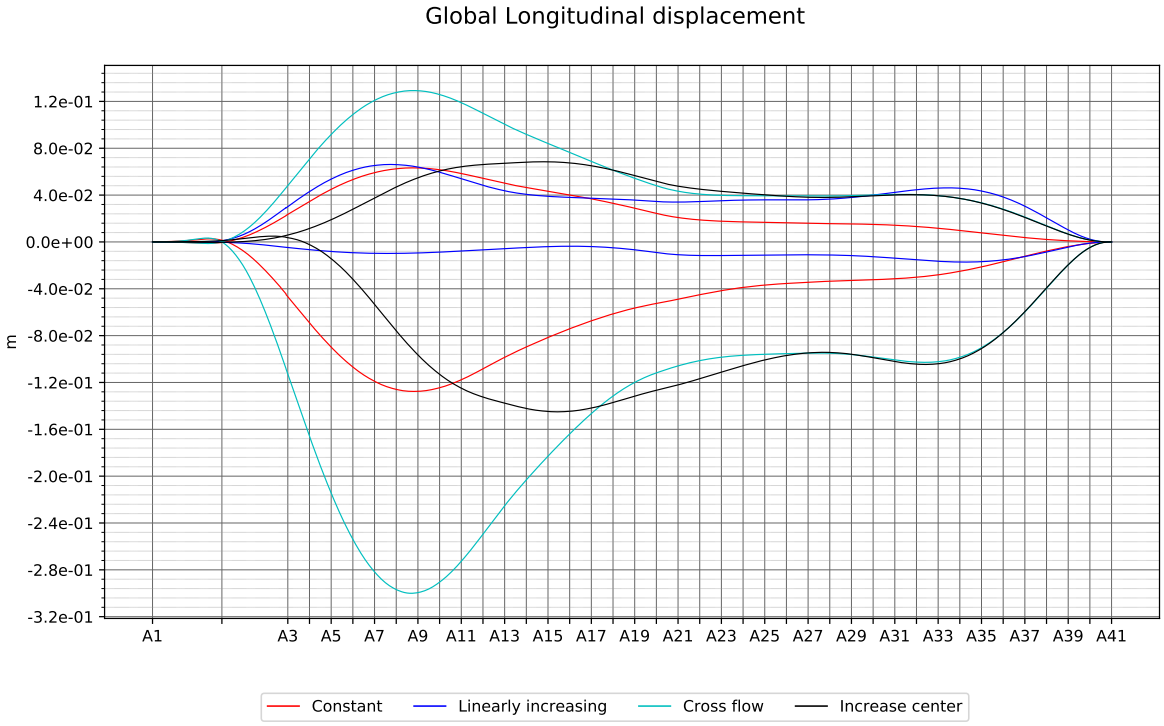

1.8 Global Transverse displacement

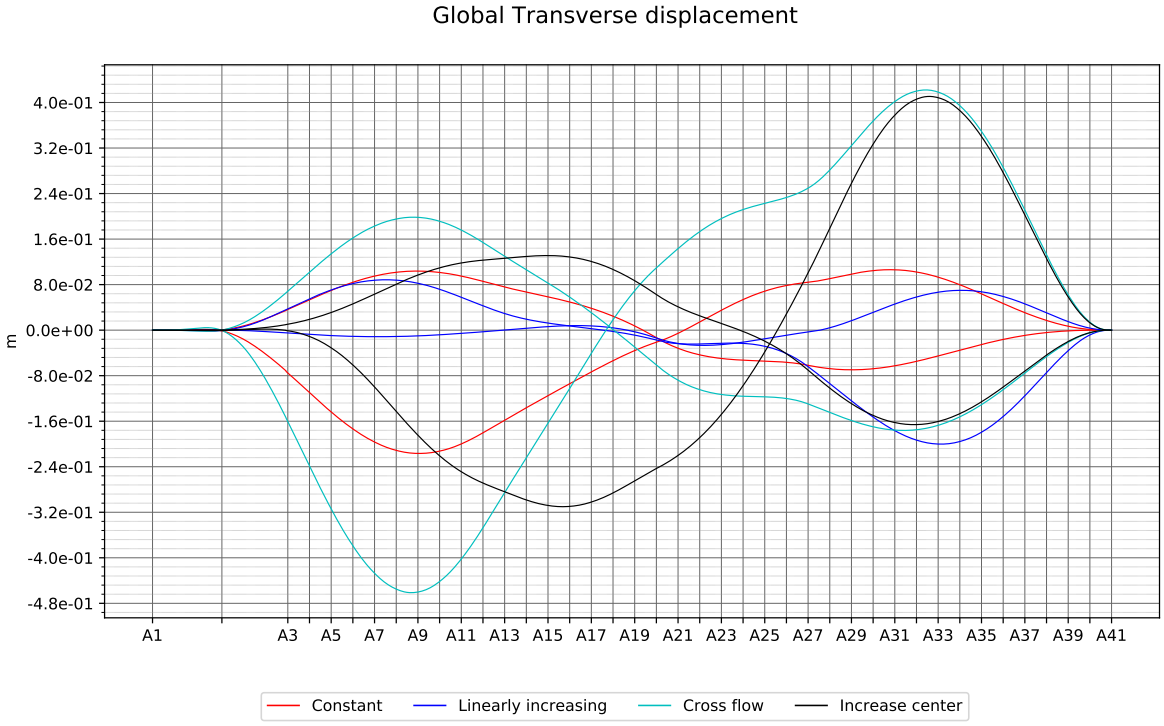

1.9 Global Vertical displacement

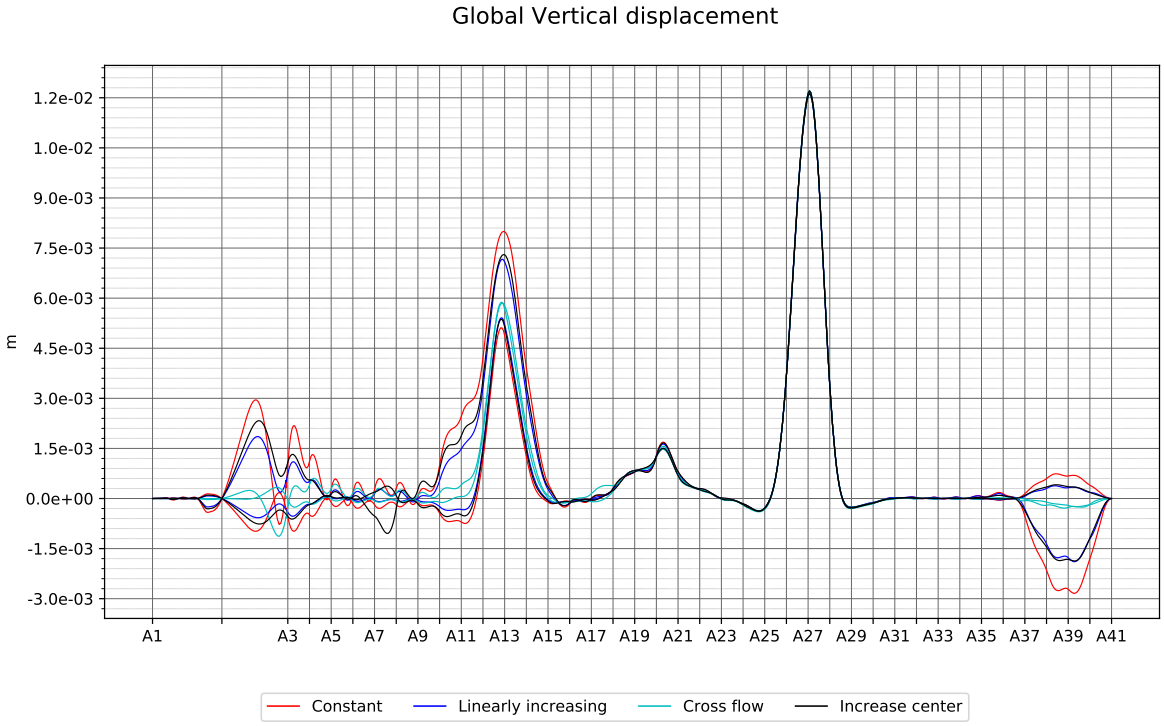

1.10 Rotation about vertical axis

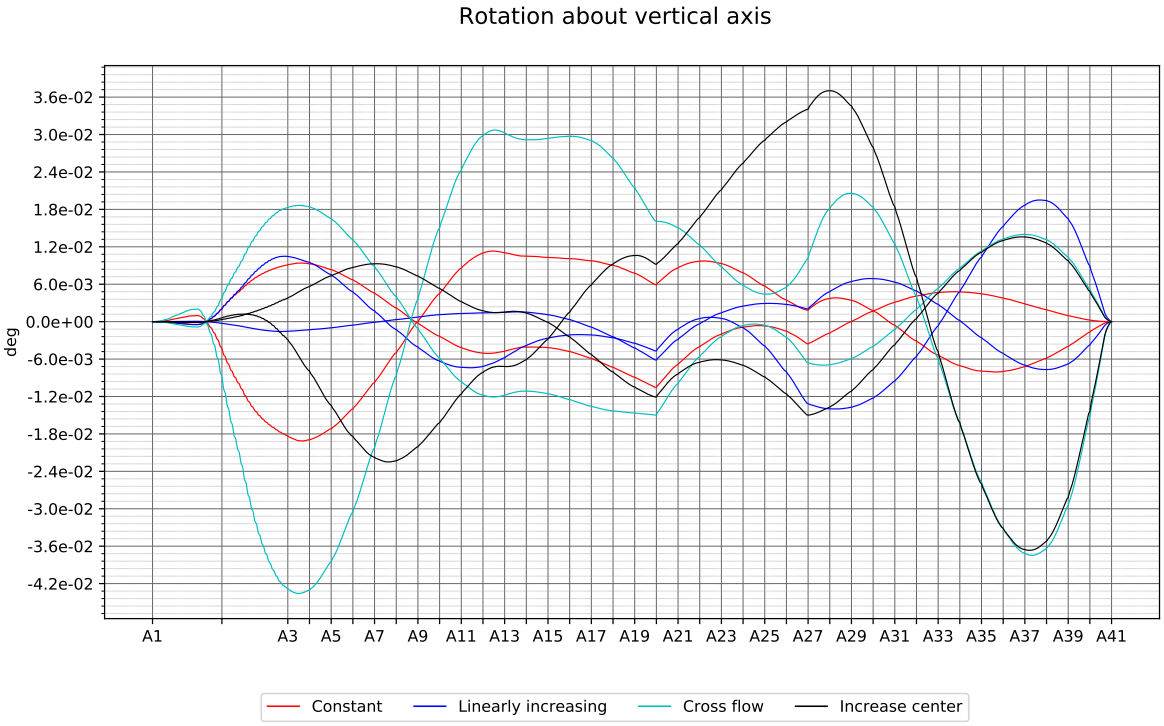

1.11 Rotation about transverse axis

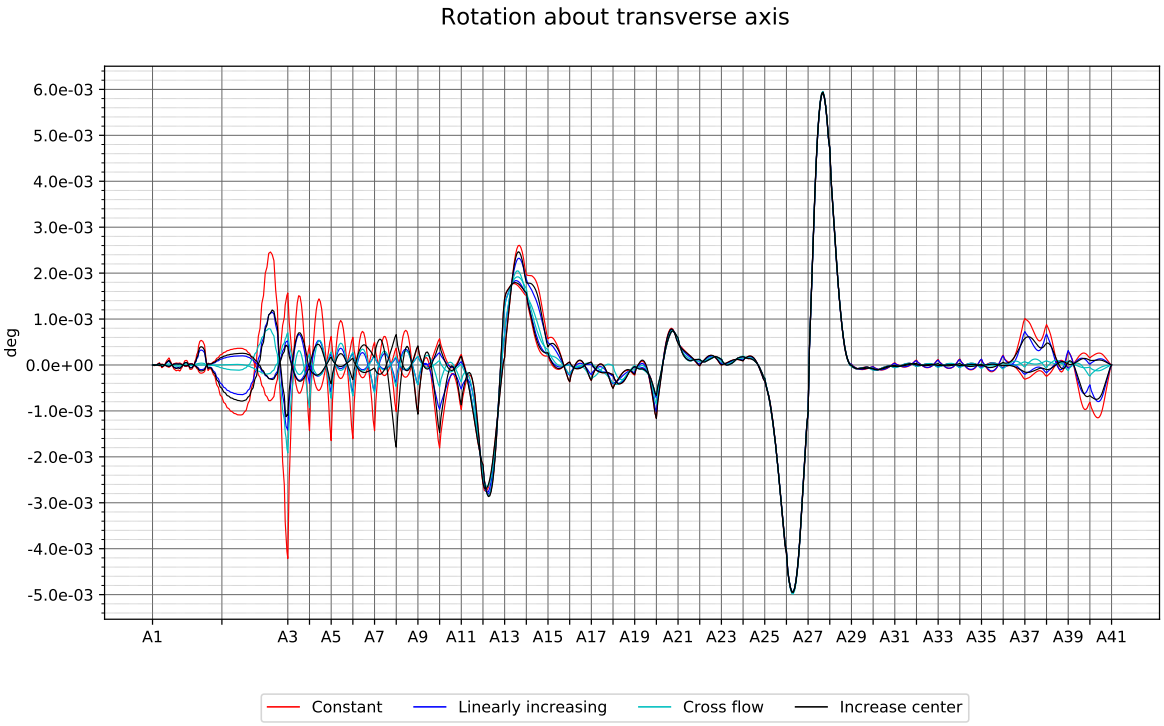

1.12 Rotation about bridge axis